南京，第十二届分子标志与核医学靶向诊断治疗大会，2017.9.9

心血管分子显像的进展

何作祥

国家心血管病中心

国家心血管疾病临床医学研究中心

心血管疾病国家重点实验室

中国医学科学院阜外心血管病医院

Molecular Imaging in Cardiovascular Diseases

- Evaluation of myocardial viability and ischemic memory
- Imaging of Cardiomyopathy
- Imaging of the cellular inflammatory response
- Evaluation of stem therapy

Imaging of Myocardial Viability

- PET
- MRI
- Thallium
- Dobutamine Echo

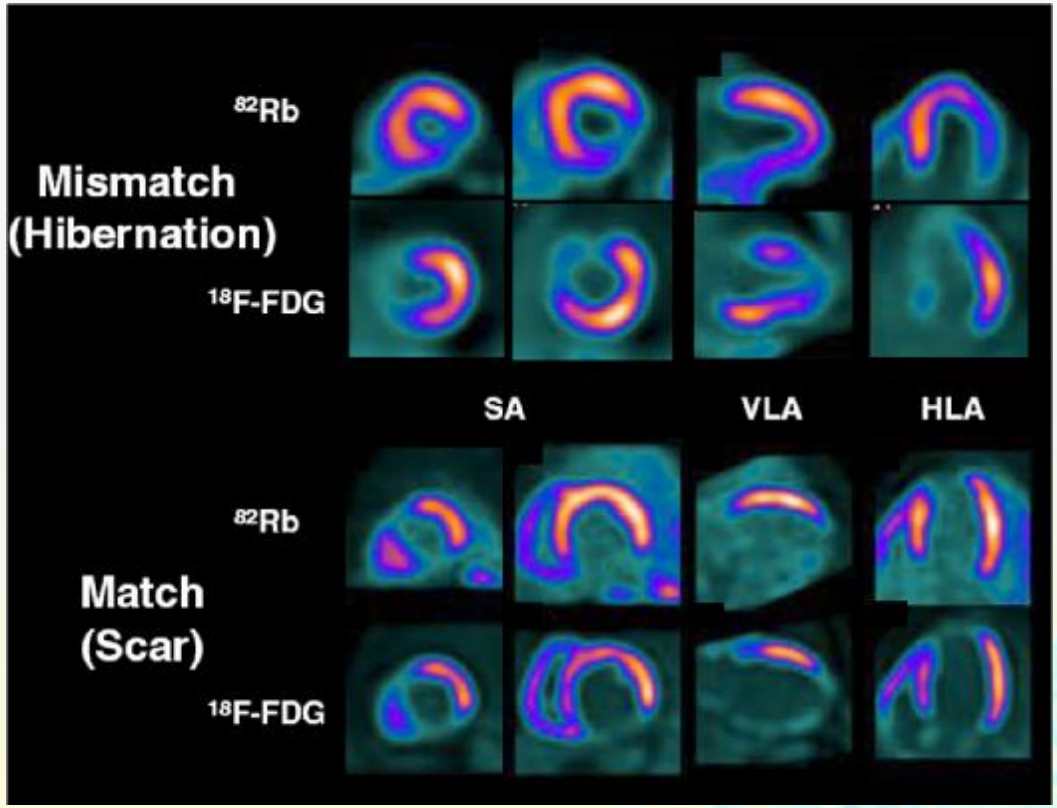

Le Guludec D, Eur J Nucl Med Mol Imaging (2008) 35:1709–1724

Survival by Viability and Treatment

93 Patients with Ischemic Cardiomyopathy and severely depressed left ventricular function

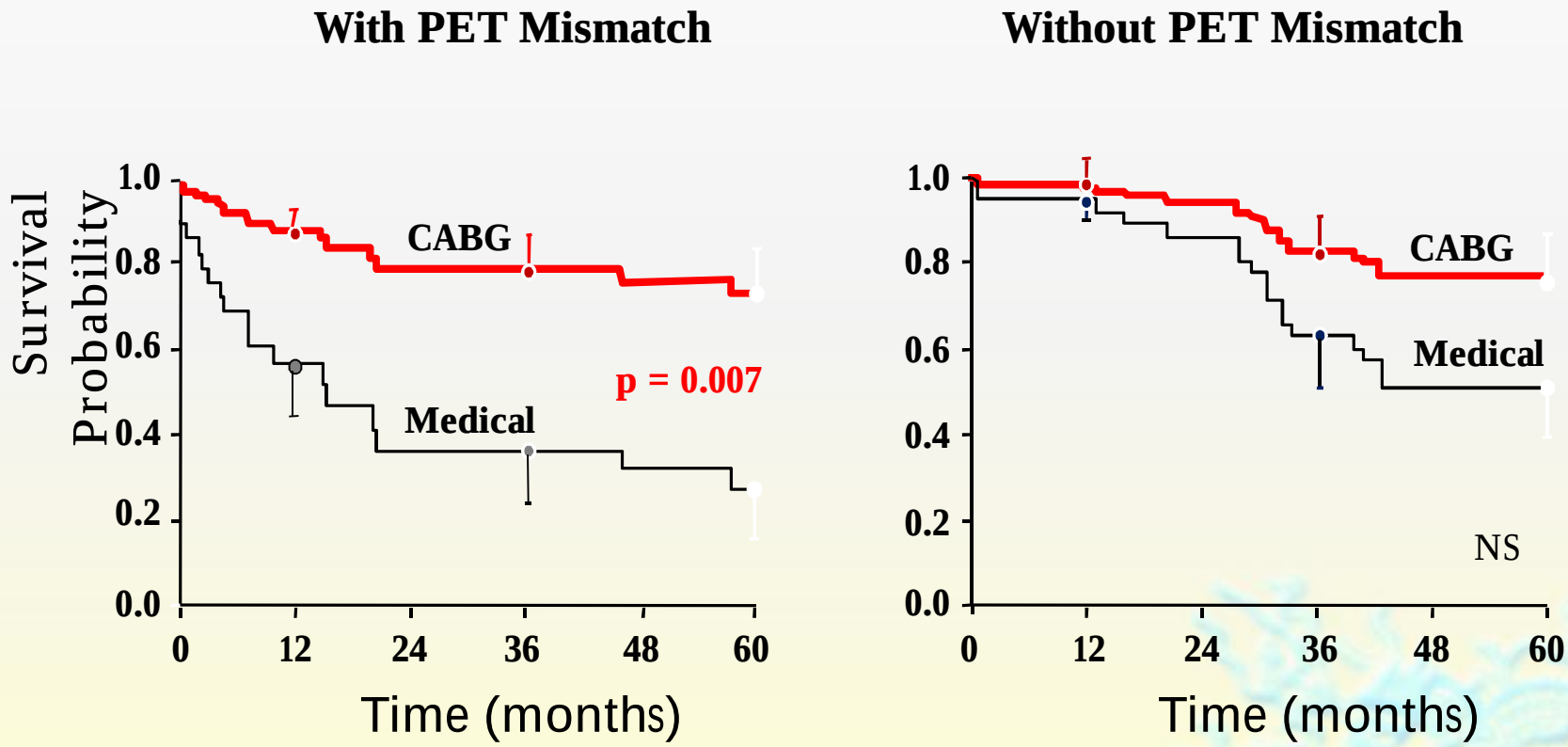

Di Carli et al, J Thor Cardiovasc Surg 1998; 116: 997

Perfusion and Metabolism Mismatch

Sestamibi

FDG

Sestamibi

FDG

Sestamibi

FDG

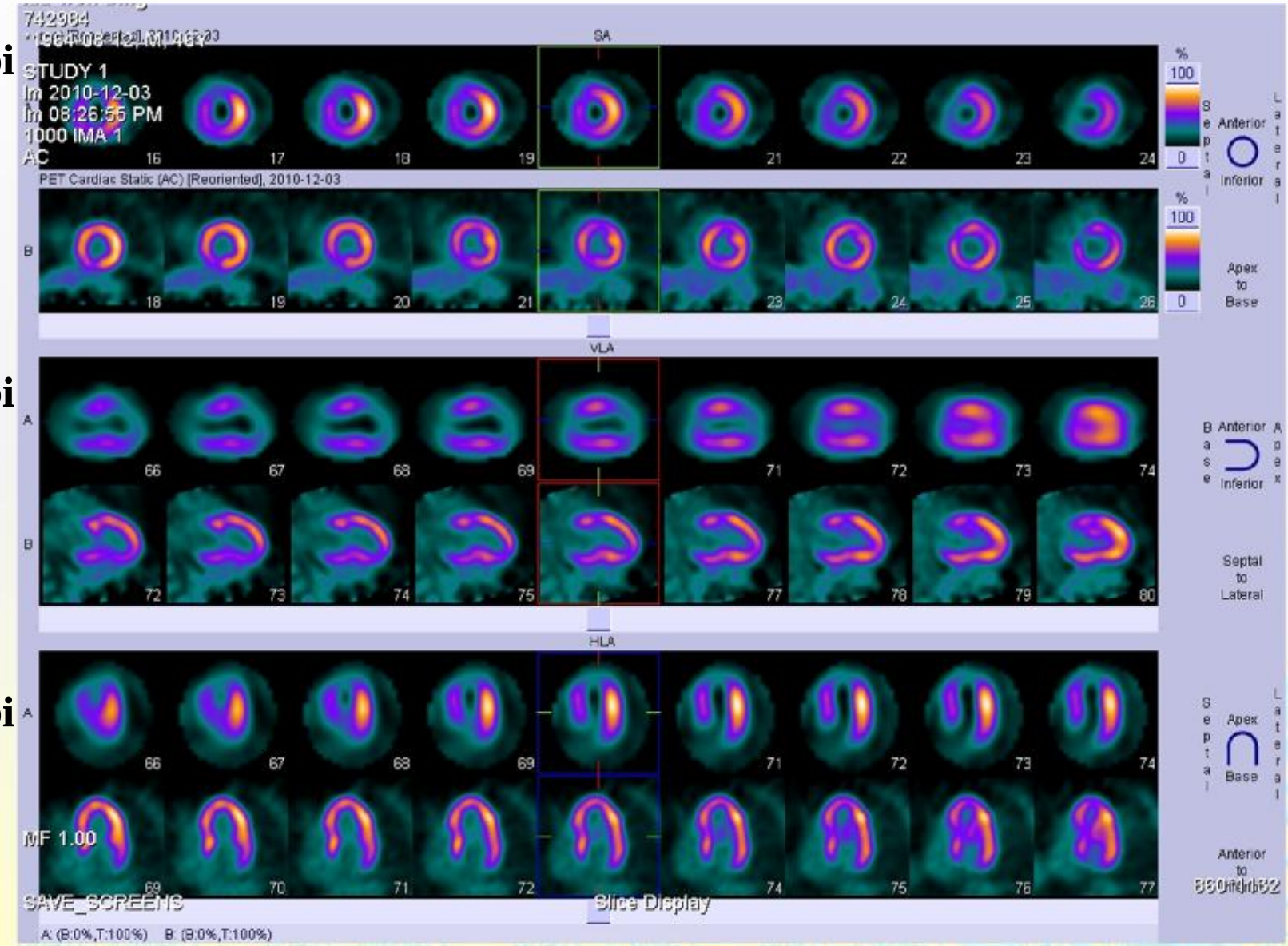

Myocardial and Metabolism Match

Sestamibi

FDG

Sestamibi

FDG

Sestamibi

FDG

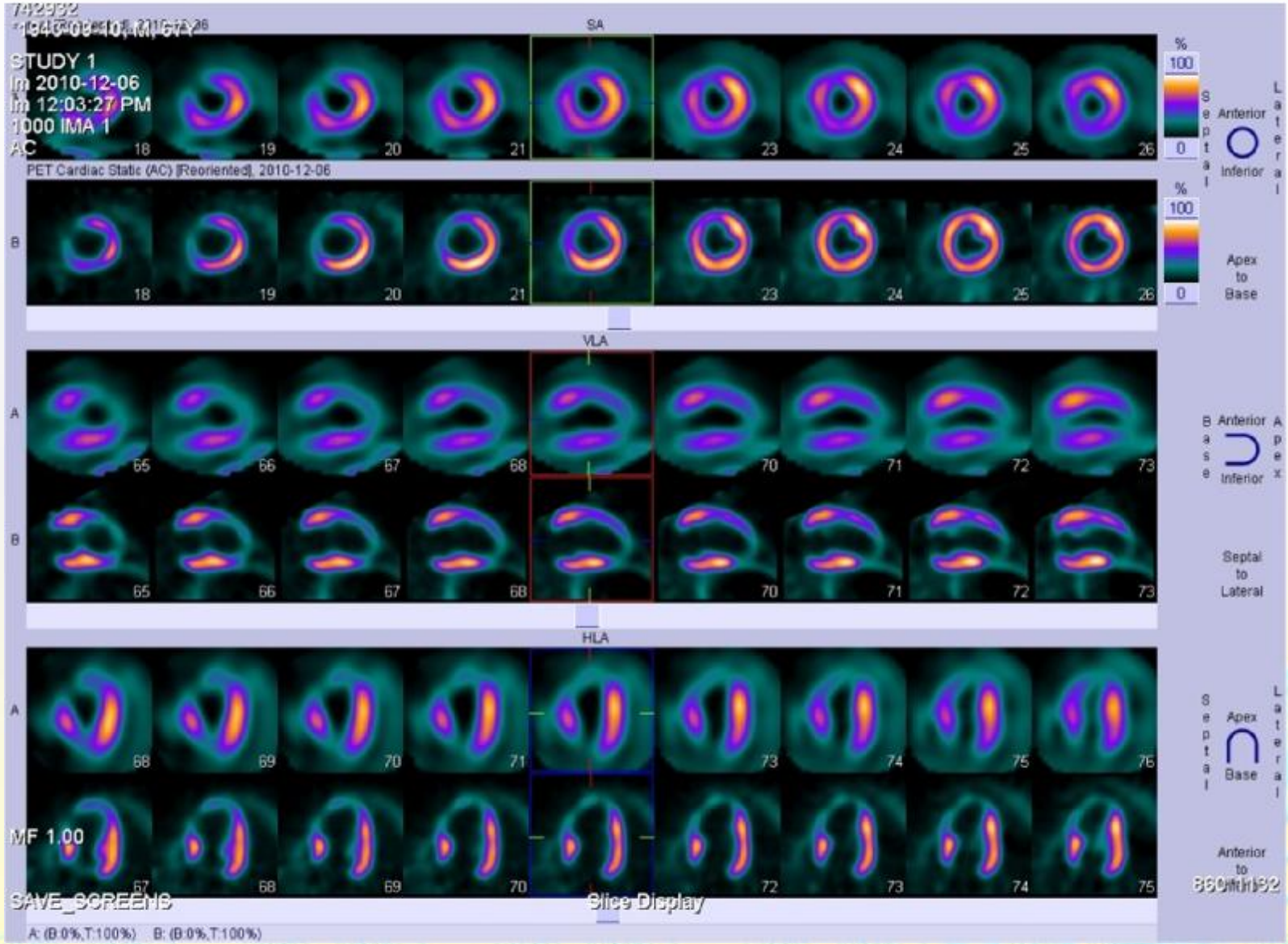

Myocardial PET/CT Imaging

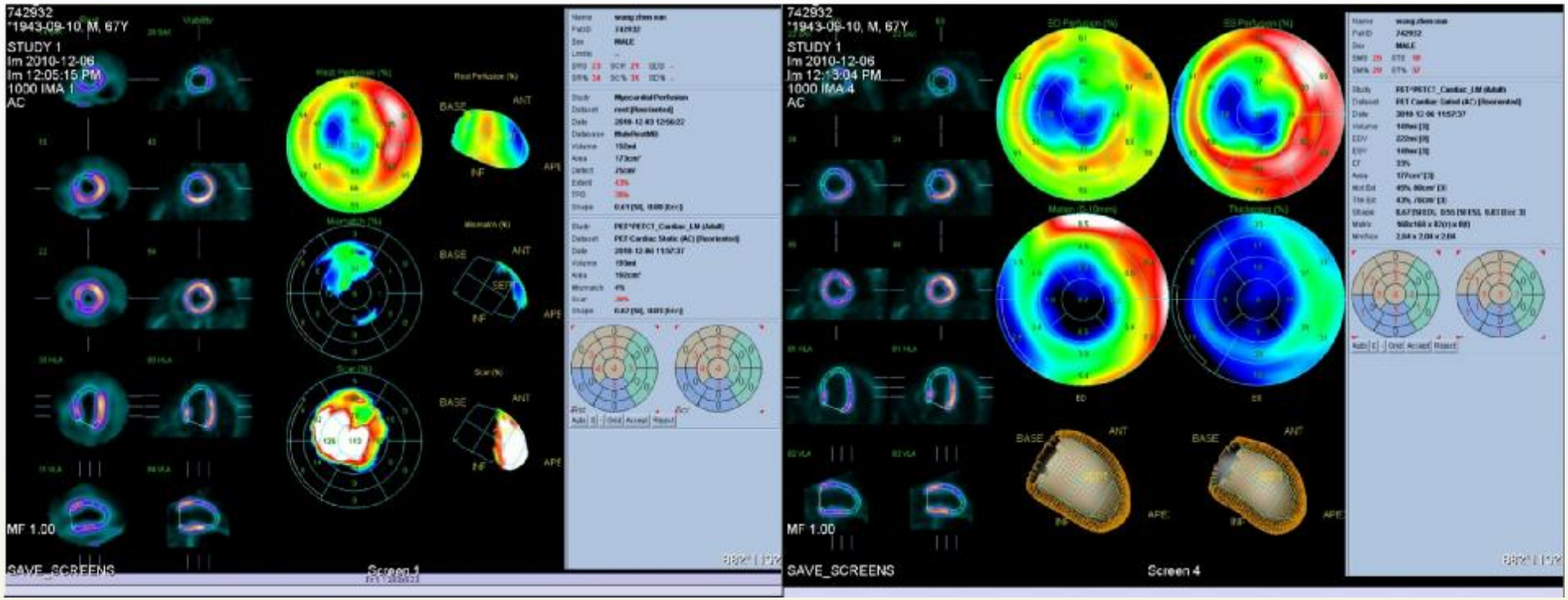

Myocardial Viability and Impact of Revascularisation in Patients with CAD and LV Dysfunction: A Meta-Analysis

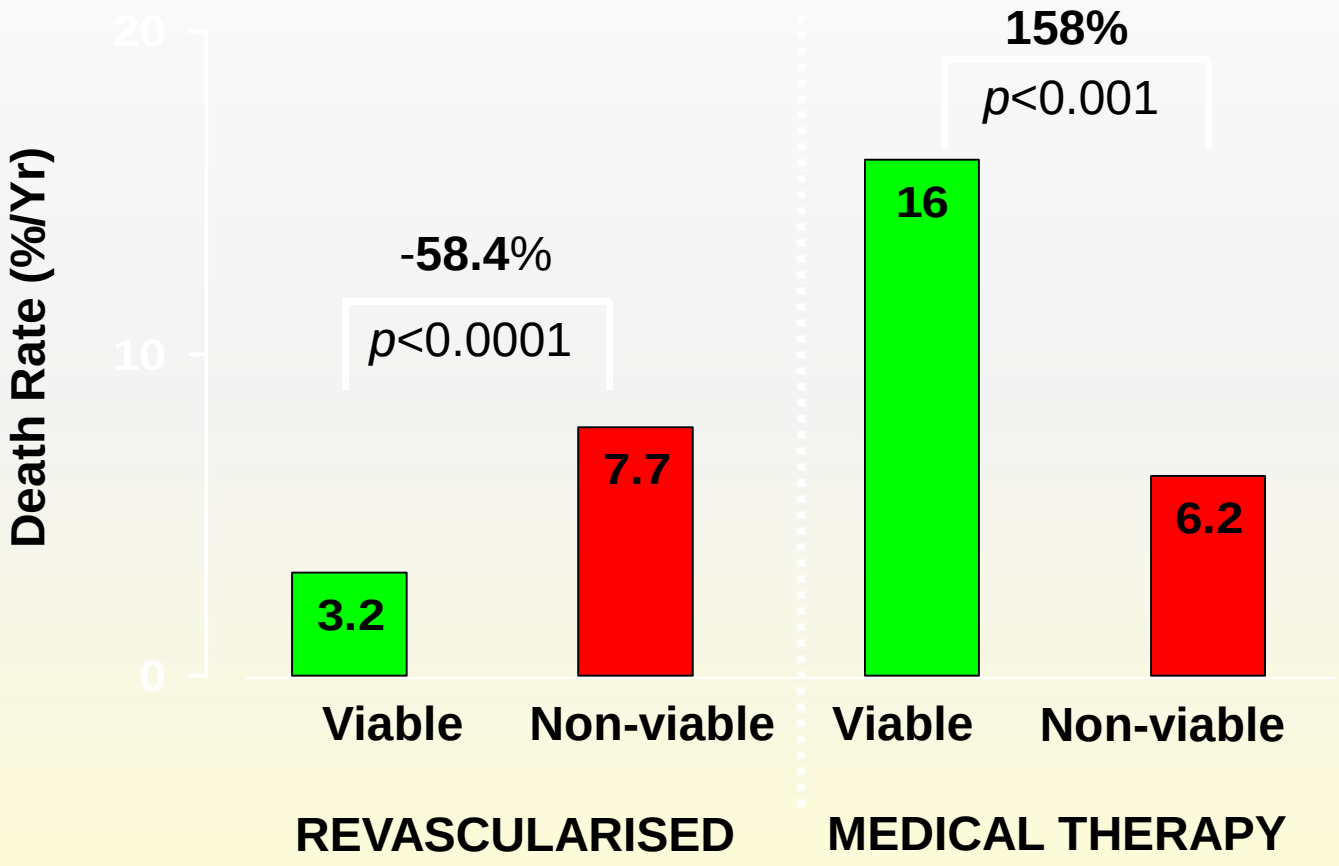

Number of studies = 24

N = 3,088

EF = 32% ± 8%

FU 25 ± 10 Mths

Allman KC, Shaw LJ, Hachamovitch R, Udelson J, JACC, 2002

Adjusted survival curves for PET and standard arms in Ottawa-FIVE and rest of PARR 2

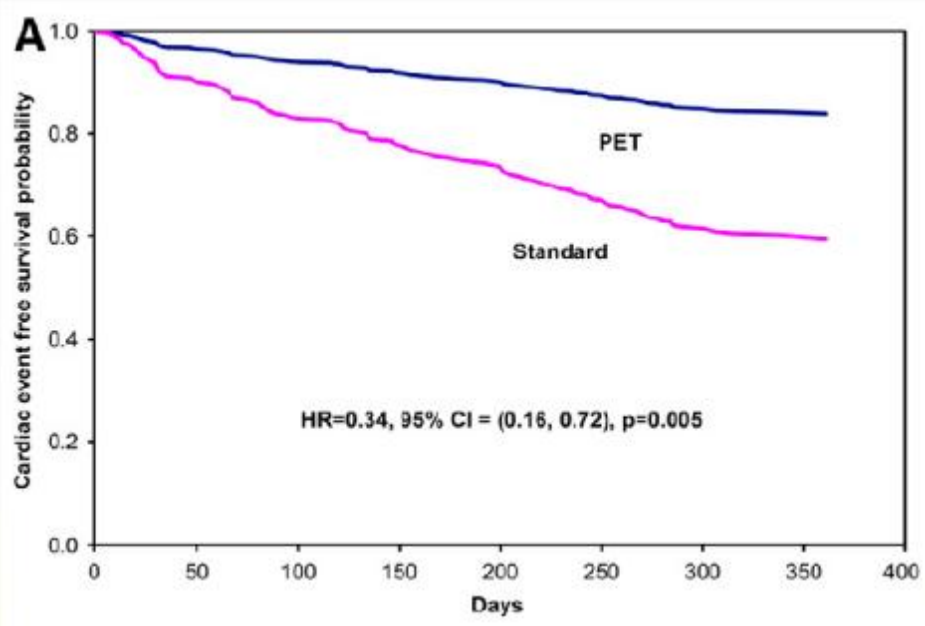

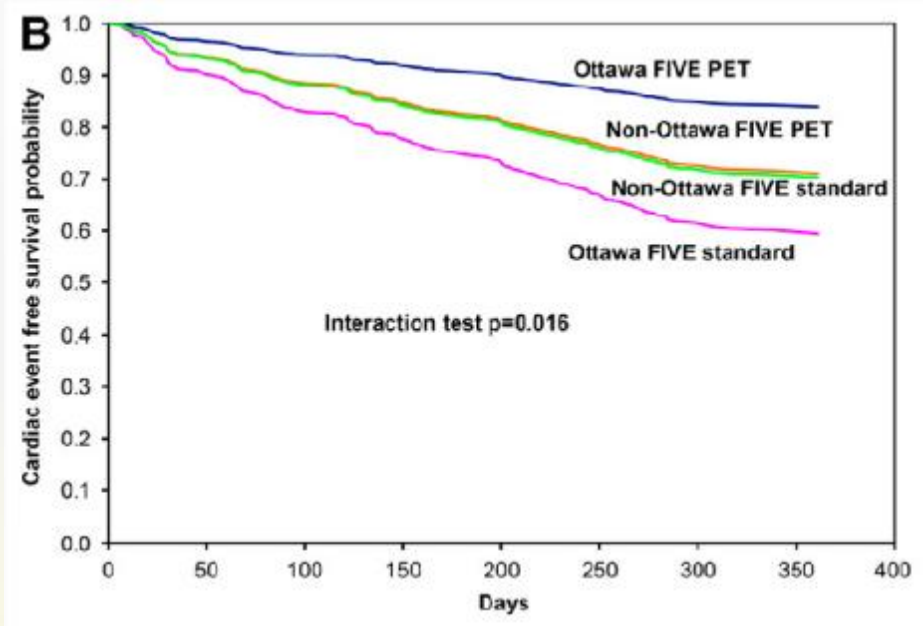

Abraham1 A, J Nucl Med 2010; 51:567–574

Myocardial Viability and Outcomes

^{18}F-FDG PET/CT

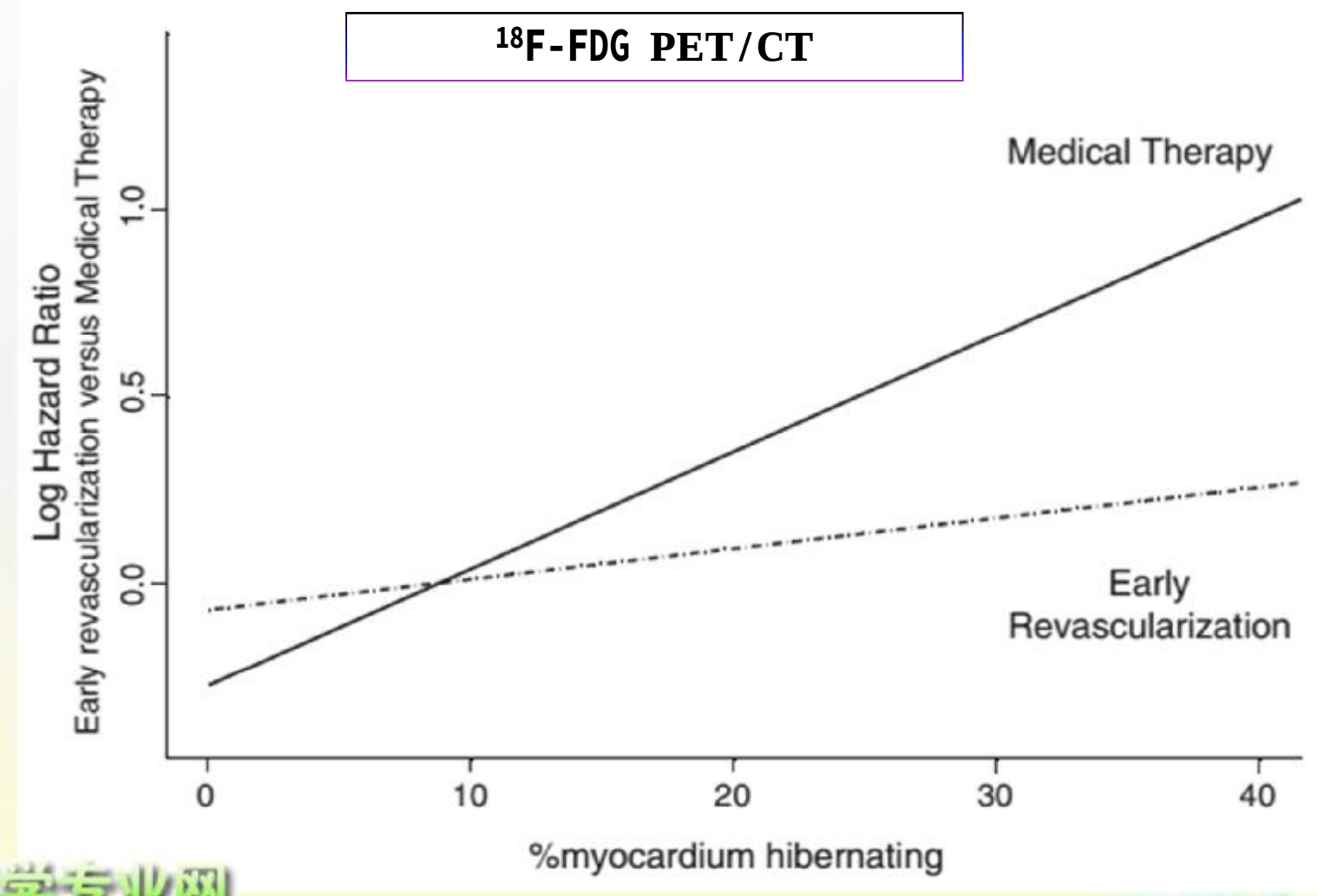

Ling LF, et al. Circ Cardiovasc Imaging. 2013;6:363-372

Identification of Therapeutic Benefit from Revascularization in Patients With LV Systolic Dysfunction

- Among patients with ischemic cardiomyopathy, hibernating, but not ischemic, myocardium identifies which patients may accrue a survival benefit with revascularization versus medical therapy.

Lee Fong Ling et al. Circ Cardiovasc Imaging. 2013;6:363-372

Direct Imaging of Exercise-Induced Myocardial Ischemia With F-18–FDG and Tc-99m-Sestamibi in Coronary Artery Disease

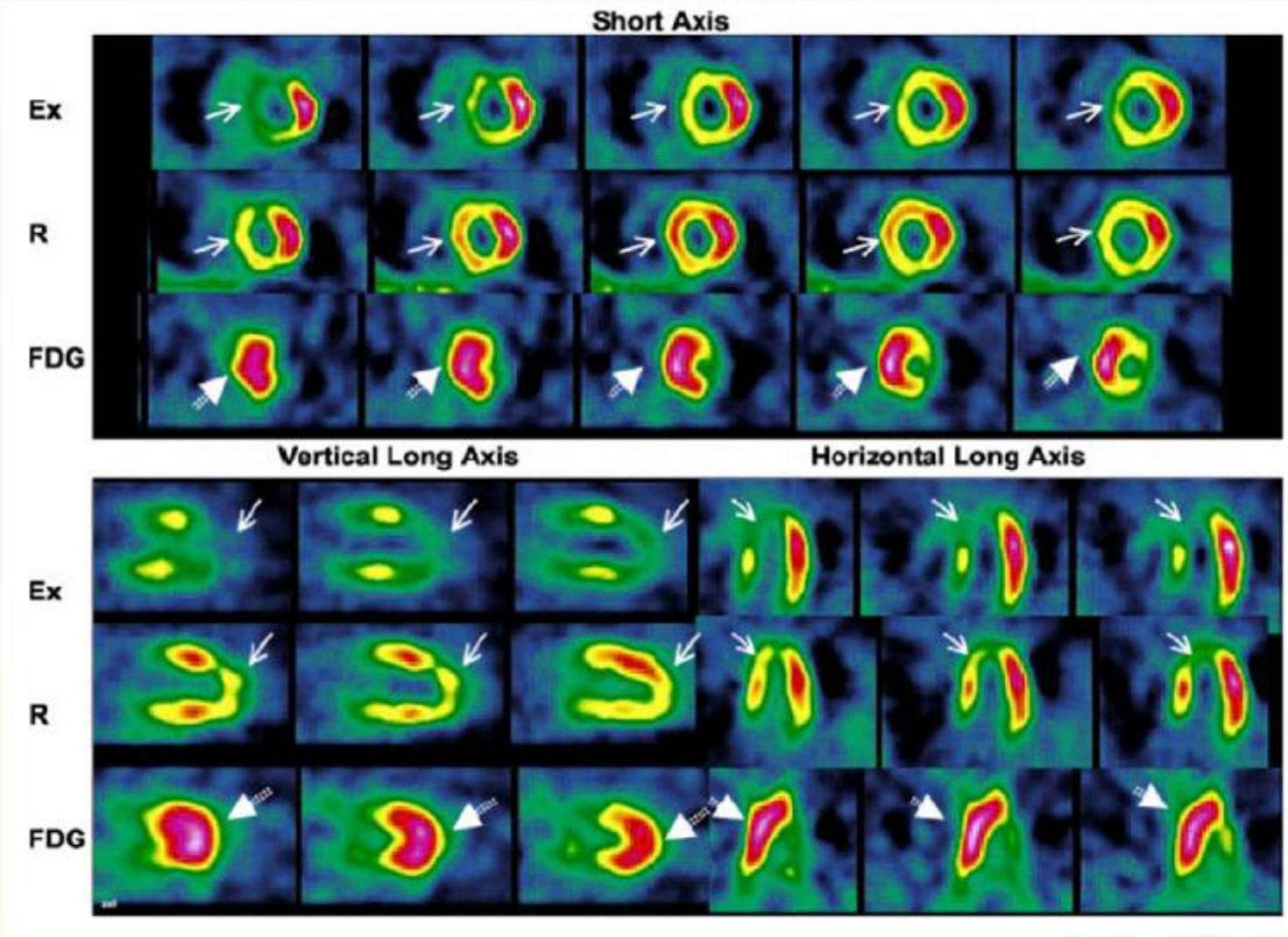

He ZX, et al. Circulation 2003

Exercise 99mTc-Tetrofosmin SPECT and FDG PET Imaging

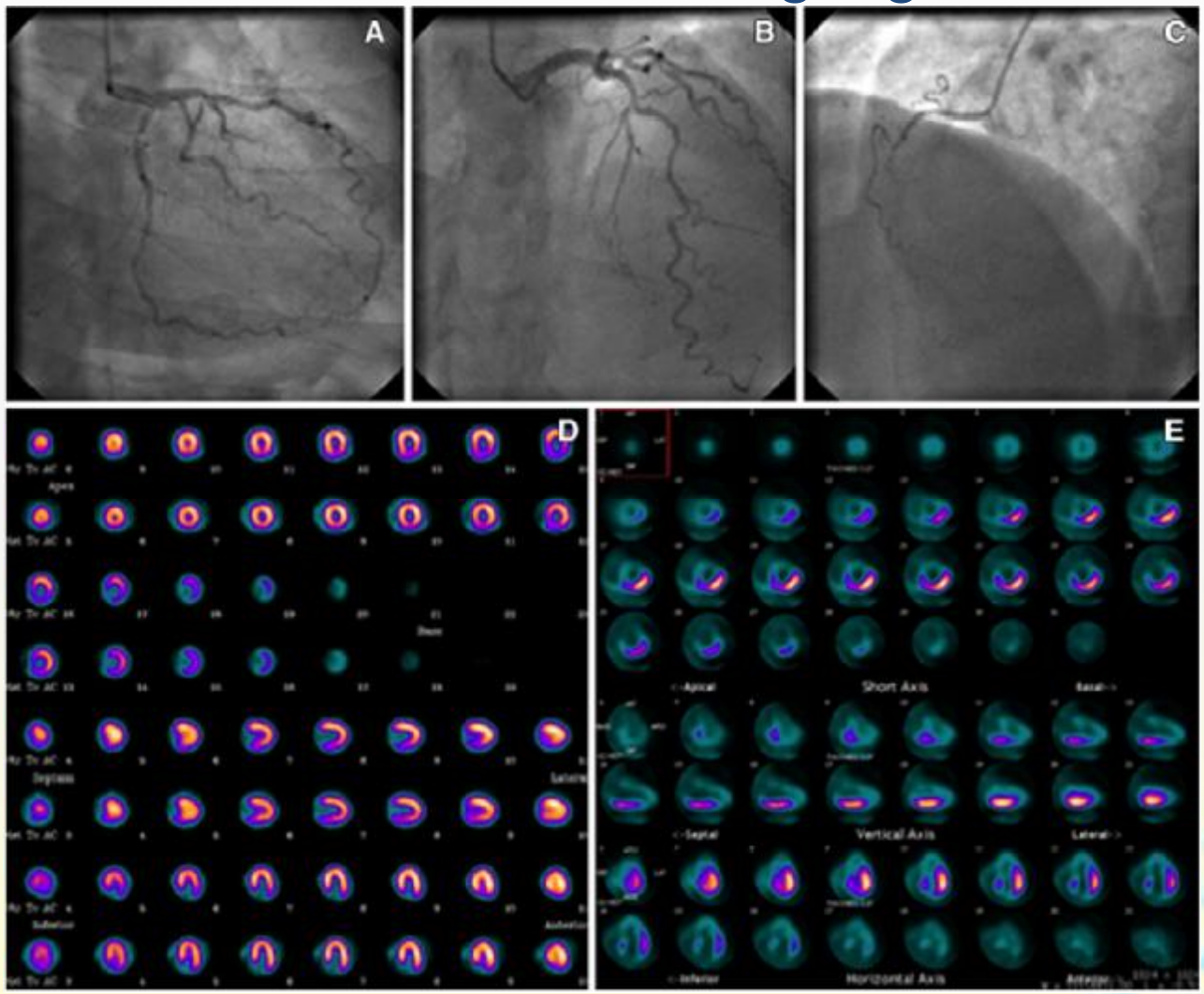

Arun S, et al. J Nucl Cardiol 2015,22:98–110
Jain D, J Nucl Cardiol 2015

Rest/Exercise FDG PET/CT

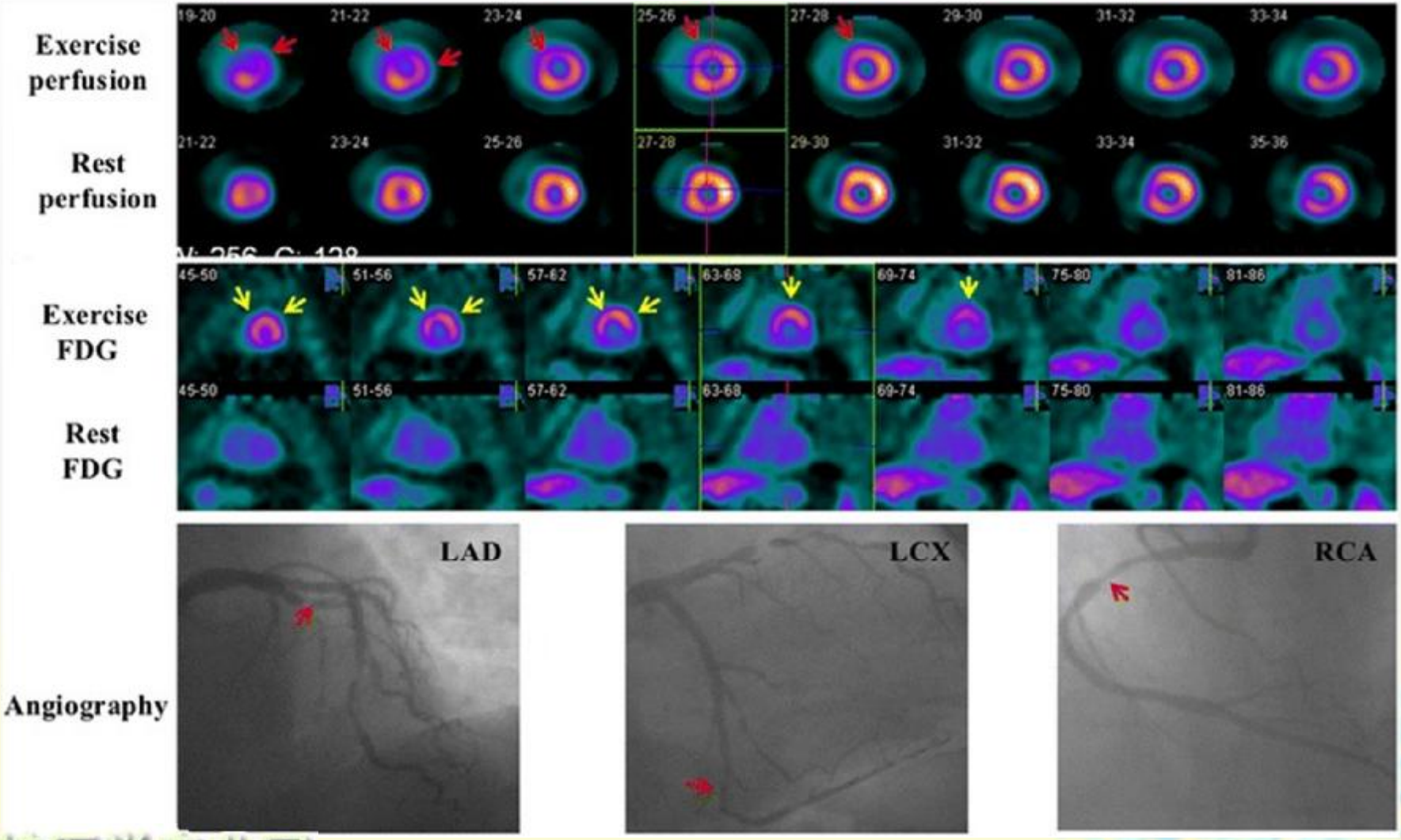

Dou et al. BMC Cardiovascular Disorders (2017) 17:120

FDG as a memory marker of transient myocardial ischaemia

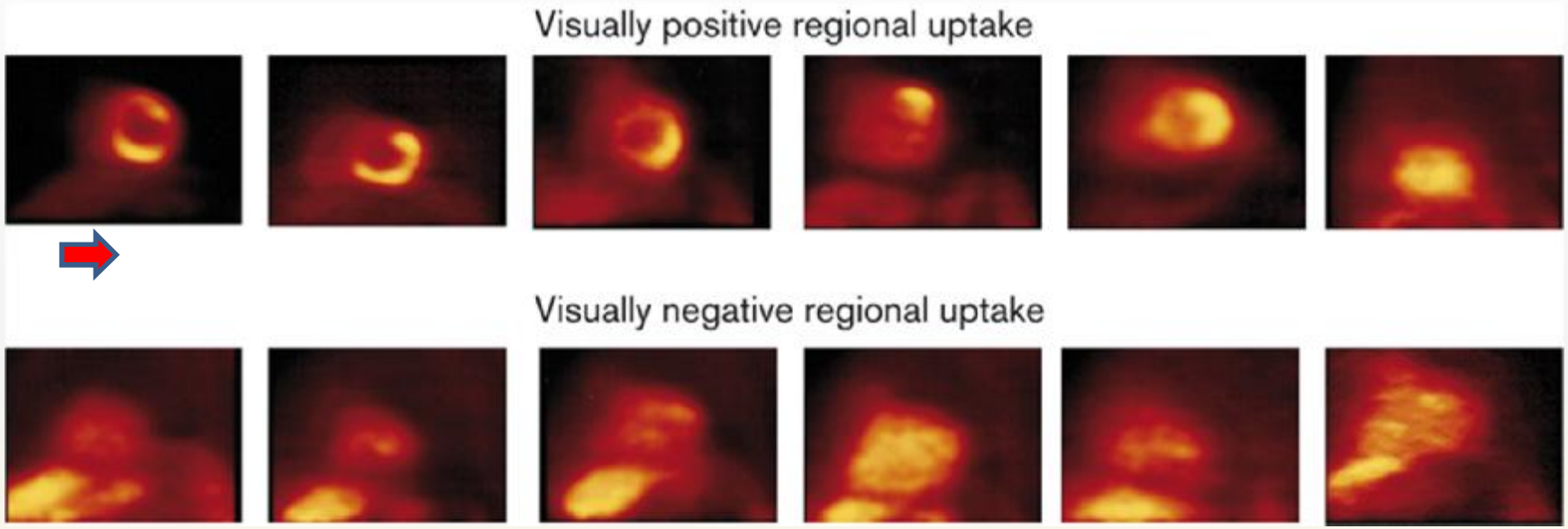

Injection of FDG 60 min after exercise

Abbott BG, et al. Nucl Med Commun 2007;28:89–94

Imaging of Ischemic Memory With FDG

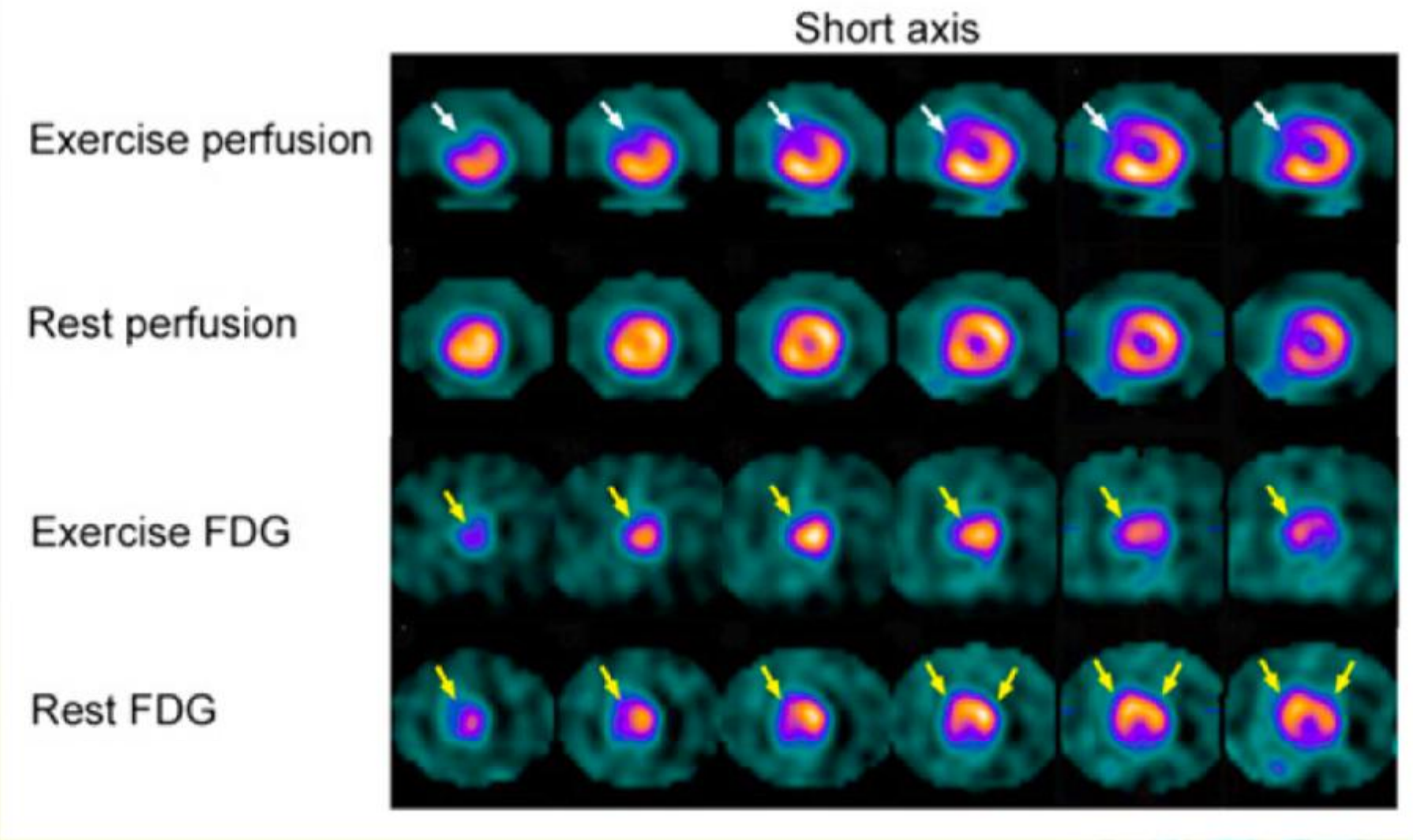

71-y-old man with exertional angina, 90% stenosis of LAD and 80% stenosis of LCx and RCA

Dou KF, Yang MF, et al. J Nucl Med 2008 ; 49:1986–1991

Rest ^{99m}Tc-sestamibi perfusion and ^{18}FDG images in unstable angina

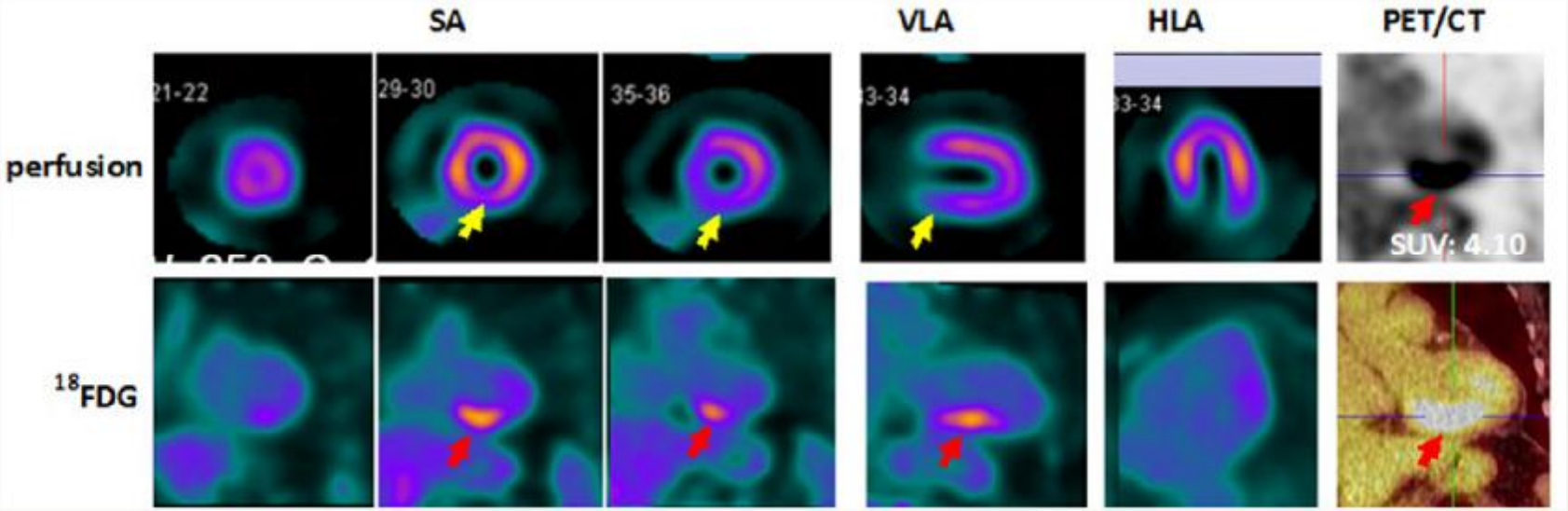

56-year-old woman with unstable angina but no history of diabetes.
Angiography: 90% stenosis of pLAD, 80% stenosis of LCx, total occlusion of pRCA.

Yang MF, et al. Curr Cardiovasc Imaging Rep, 2012
Dou KF, et al. Nucl Med Comm, 2015

Rest ^{99m}Tc-sestamibi perfusion and ^{18}FDG images in unstable angina

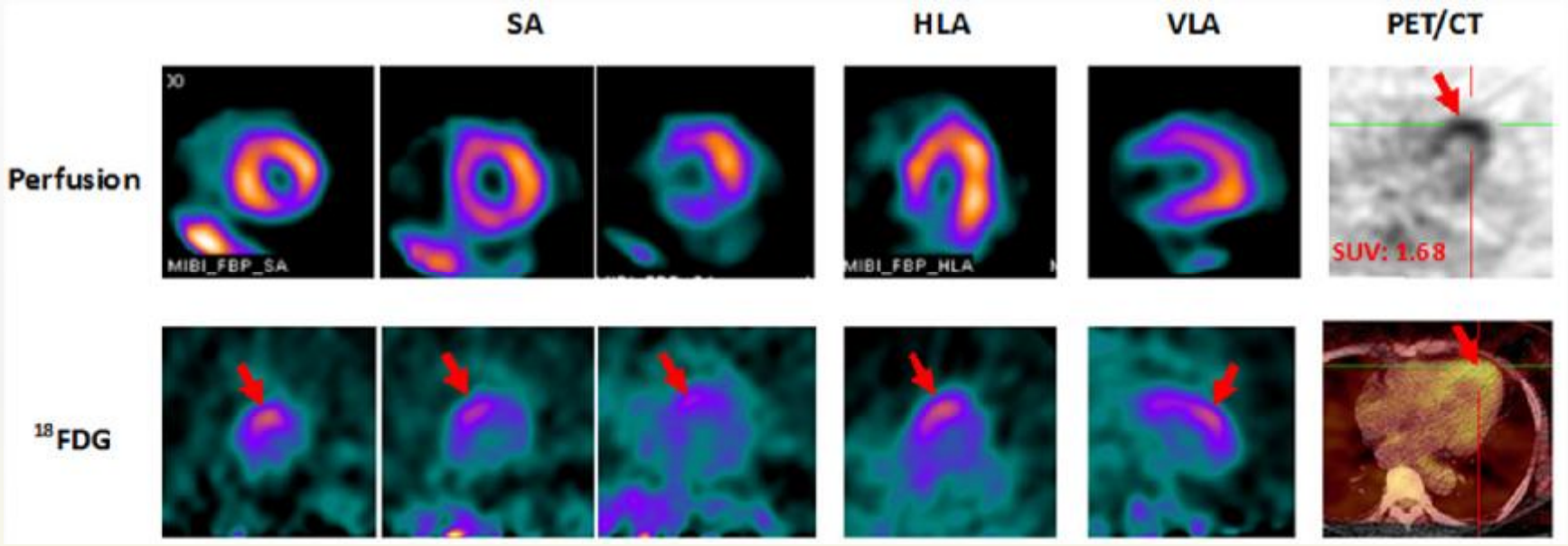

56-year-old woman with unstable angina and a history of diabetes.
Angiography: 90% stenosis of pLAD, 90% stenosis of dRCA

Yang MF, et al. Curr Cardiovasc Imaging Rep, 2012
Dou KF, et al. Nucl Med Comm, 2015

Perfusion SPECT and FDG PET in DCM and HF

Sestamibi

FDG

Sestamibi

FDG

Sestamibi

FDG

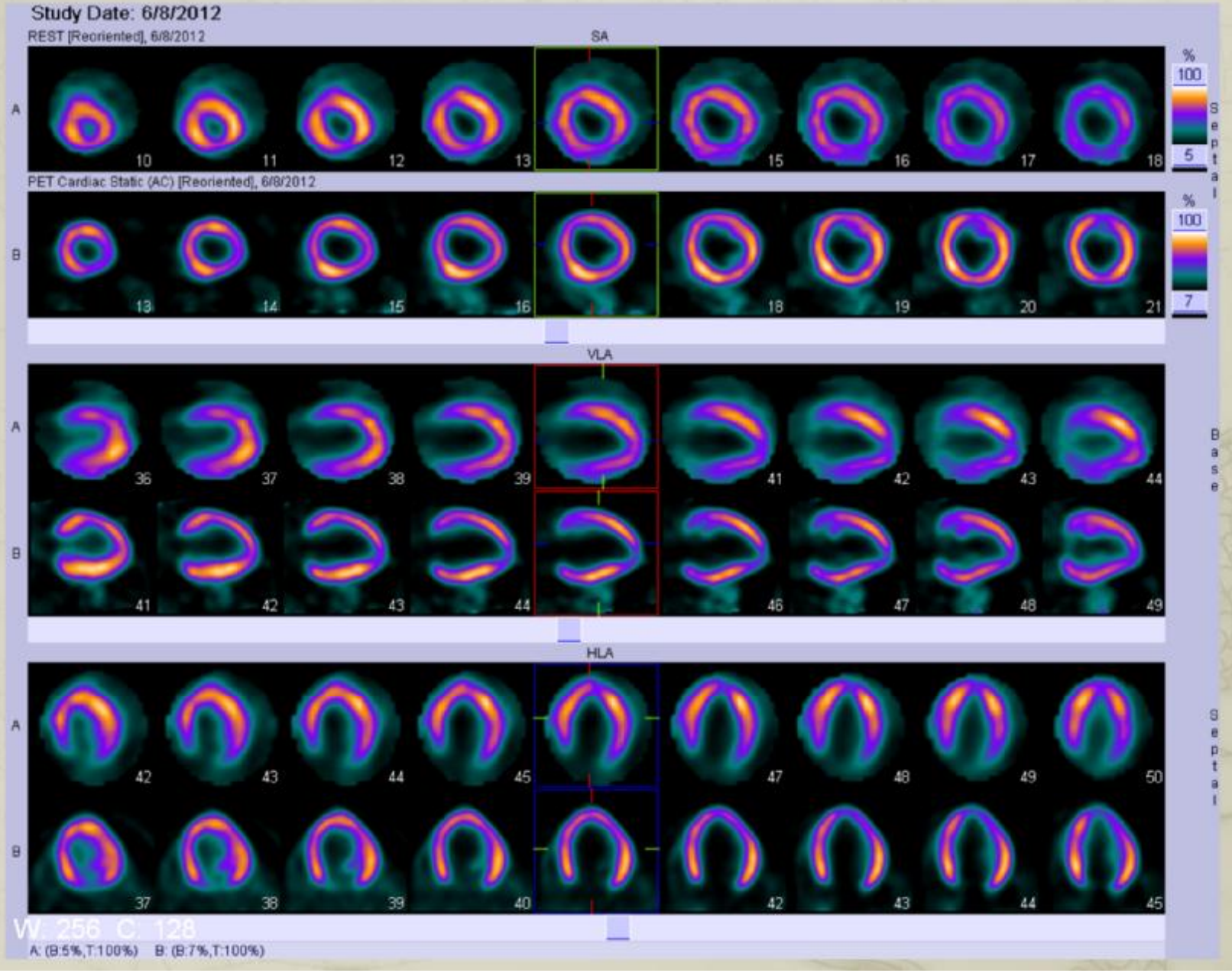

Regional wall motion in DCM by gated SPECT and cardiac MRI (n = 36)

	Cine MRI		
Gated SPECT	**Severe hypokinesia**	**Akinesia or dyskinesia**	**Total**
Severe hypokinesia	**555**	**9**	**564**
Akinesia or dyskinesia	**24**	**24**	**48**
Total	**579**	**33**	**612**

Wang F, et al. Eur J Nucl Med Mol Imaging 2009; 36:1611–1621

Dilated Cardiomyopathy

TABLE 3. The Comparison of LGEs and Perfusion/Metabolism Patterns in 42 Patients With IDCM (714 Segments)

	Perfusion/Metabolism				
cMRI	Normal	Mismatch	Mild-to-Moderate Match	Severe Match	Total
Non-LGE	526	63	12	9	610
Mid-wall LGE	44	5	7	6	62
Transmural LGE	12	15	3	12	42
Total	582	83	22	27	714

Wang L, *Clin Nucl Med* 2012; 37: 1163-1169

Rest myocardial perfusion defect predicts cardiac death in patients with DCM and HF

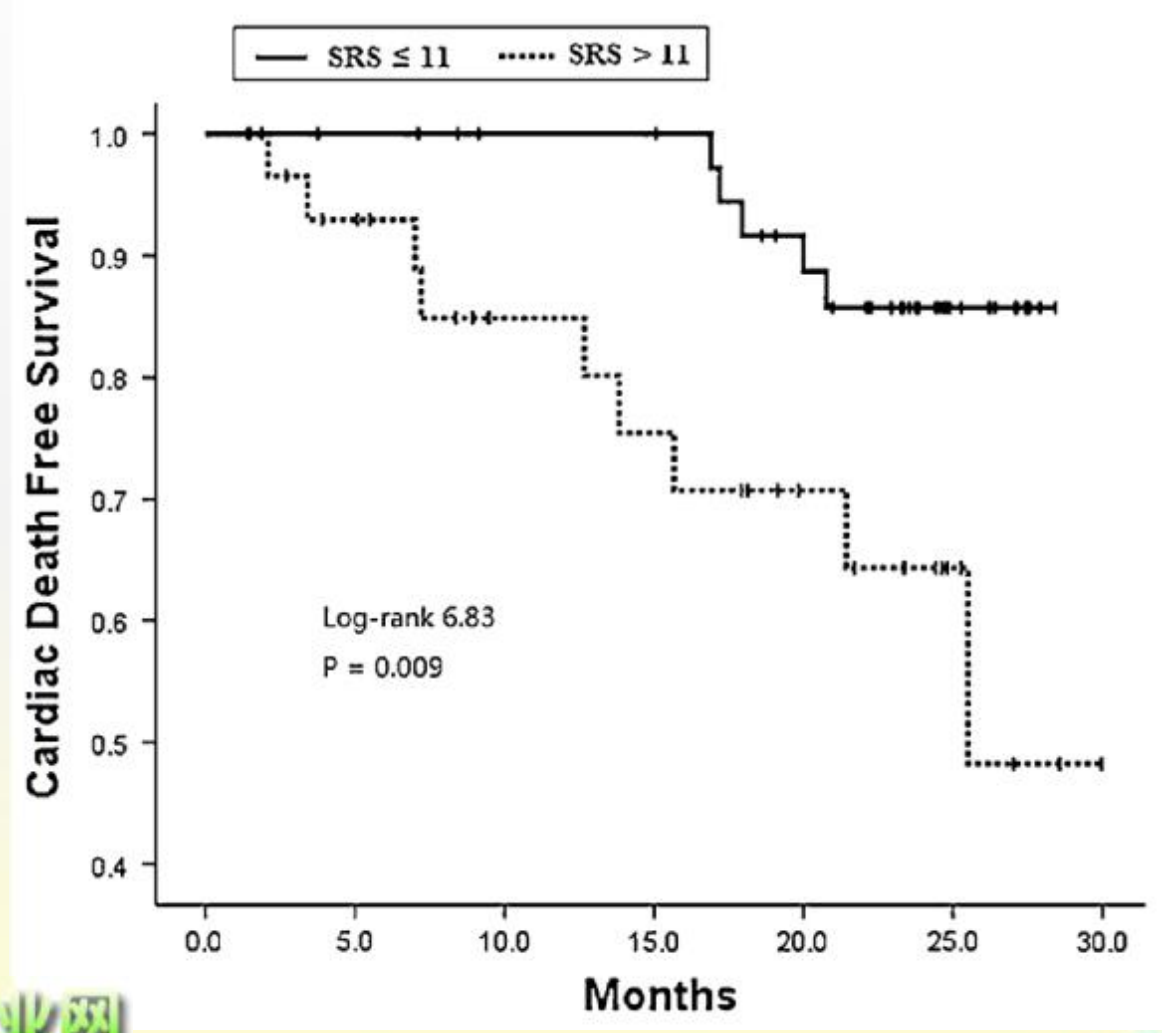

Cai M, et al. Int J Cardiovasv Imaging 2012

Kaplan-Meier survival according to the presence of Perfusion Metabolism Mismatch in DCM and HF

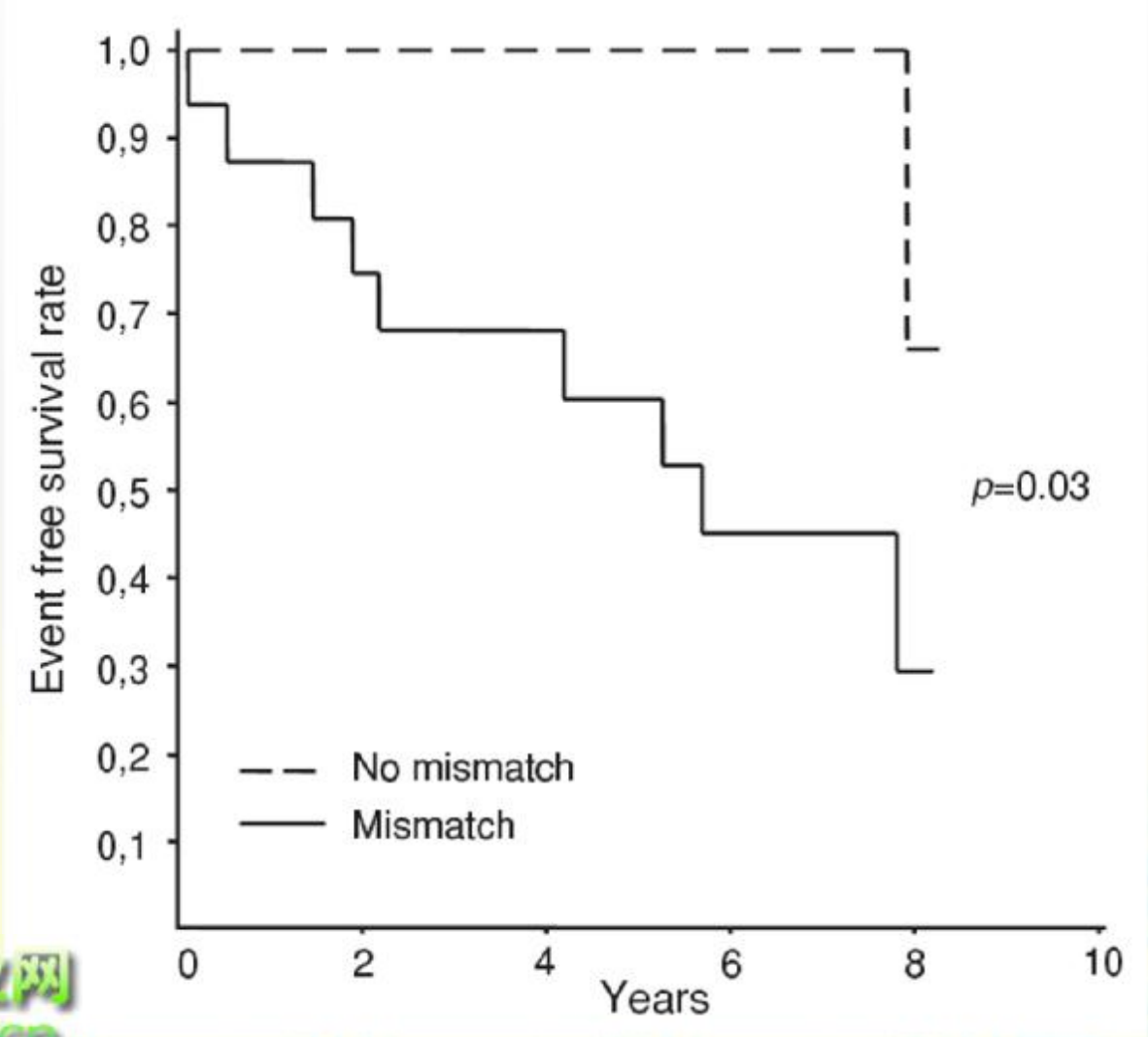

J Nucl Cardiol 2009;16:769–74

Septal Reverse Perfusion and Metabolism Mismatch in DCM and LBBB

Sestamibi

FDG

Sestamibi

FDG

Sestamibi

FDG

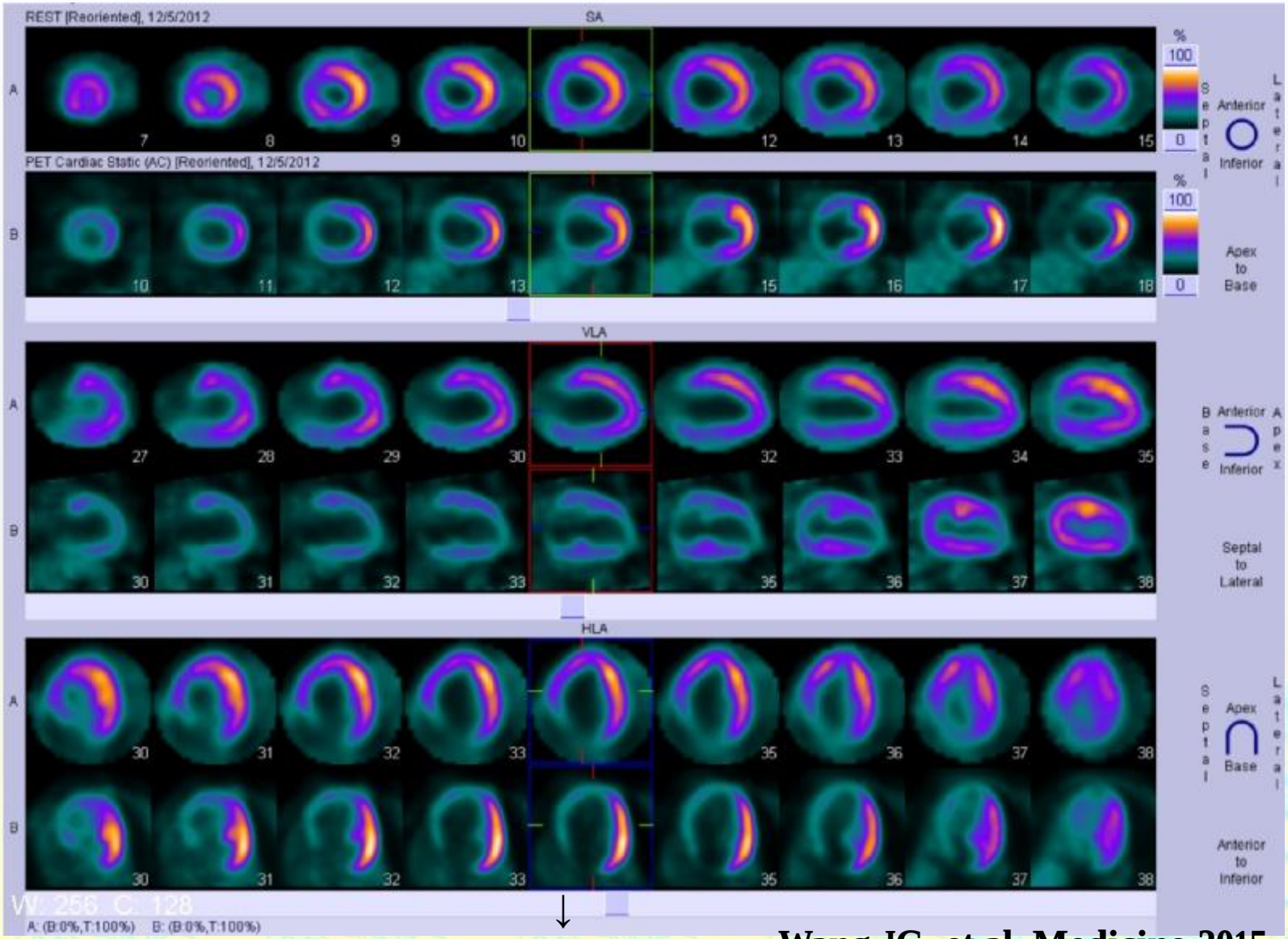

Wang JG, et al. Medicine 2015

Dilated Cardiomyopathy

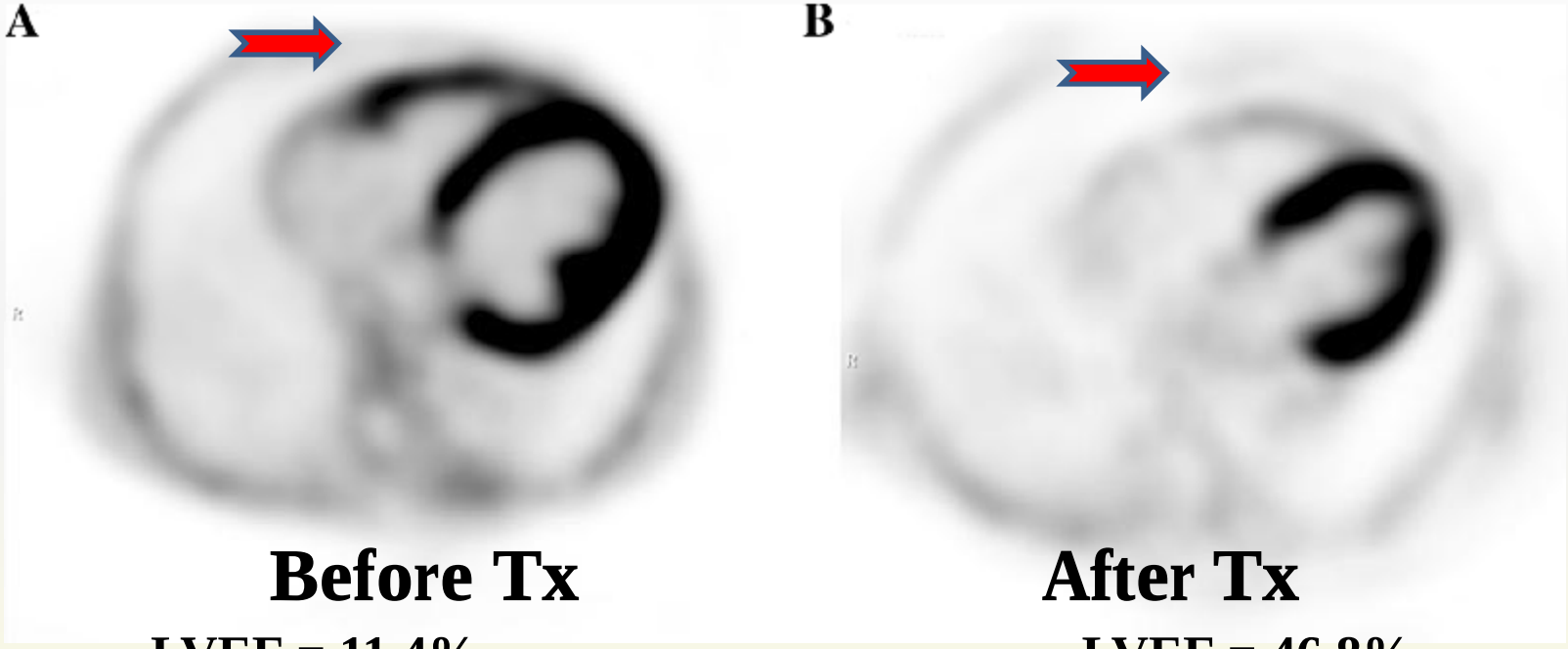

Before Tx

LVEF = 11.4%
RVEF = 13.3%
cRVSUV = 7.12
cR/L = 0.80

After Tx

LVEF = 46.8%
RVEF = 34.0%
cRVSUV = 2.55
cR/L = 0.42

Wang L, J Nucl Cardiol 2015
Fang W, et al. Nucl Med Commun. 2010;31(11):981

Myocardial ischemia in patients with DCM

- LV regional myocardial perfusion, wall motion, and metabolism abnormalities are often present in patients with DCM.

Fang W, et al. *Nucl Med Commun.* 2010;31(11):981

Hypertrophic Cardiomyopathy

Sestamibi

FDG

Sestamibi

FDG

Sestamibi

FDG

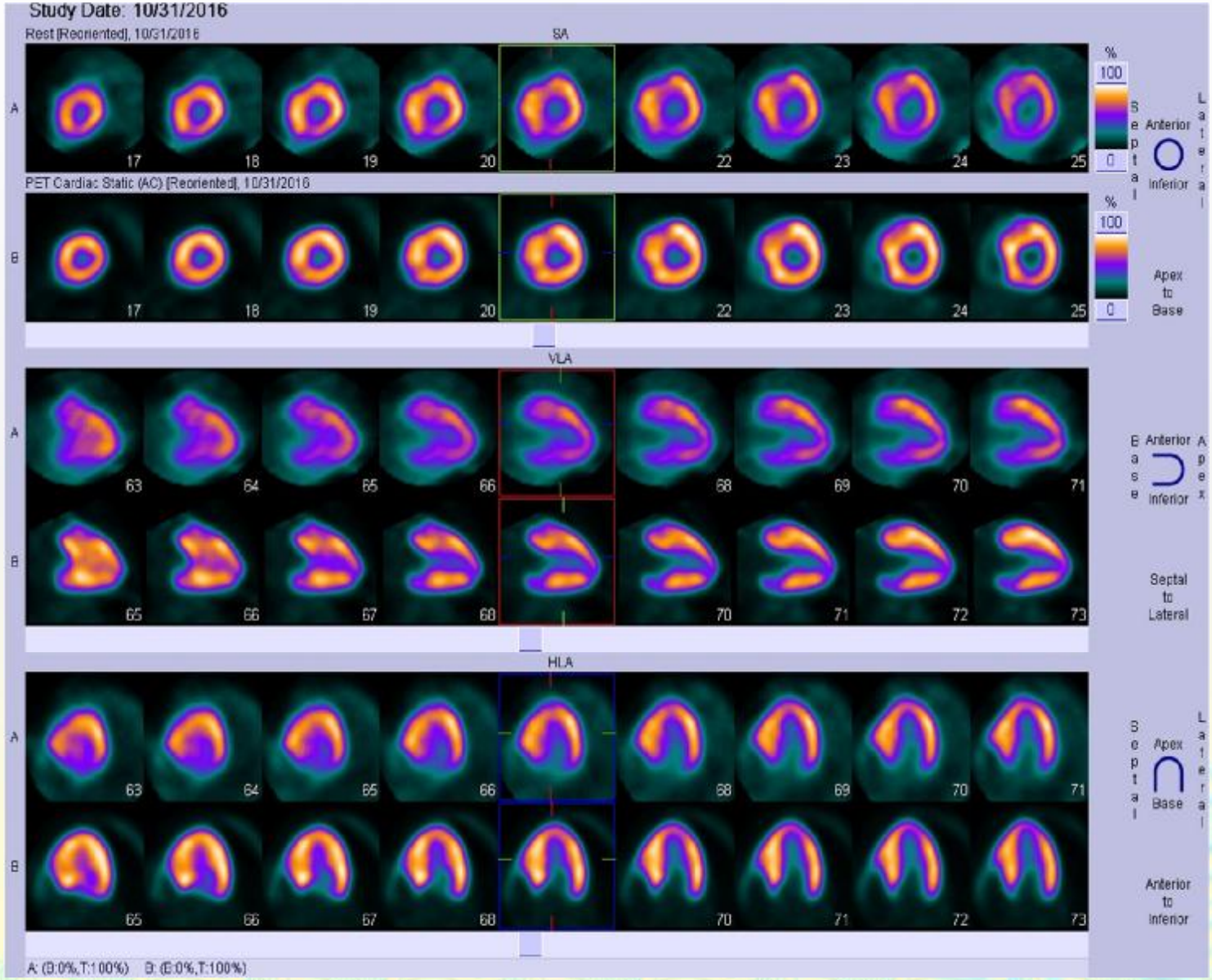

Perfusion SPECT and FDG PET in HCM

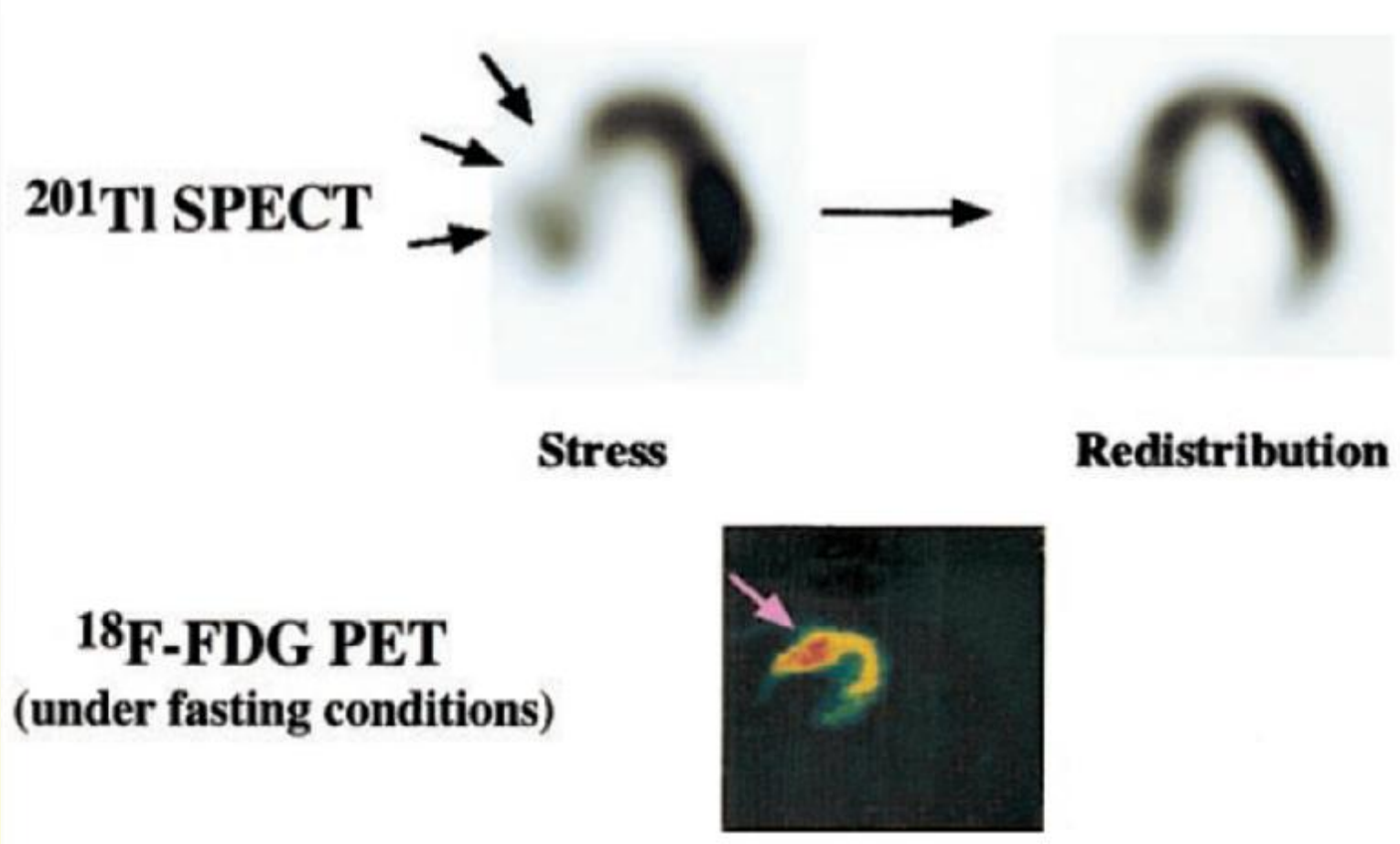

Isobe S, et al. J Nucl Med 2003; 44:1717–1724

Direct Imaging of Exercise-Induced Myocardial Ischemia in HCM

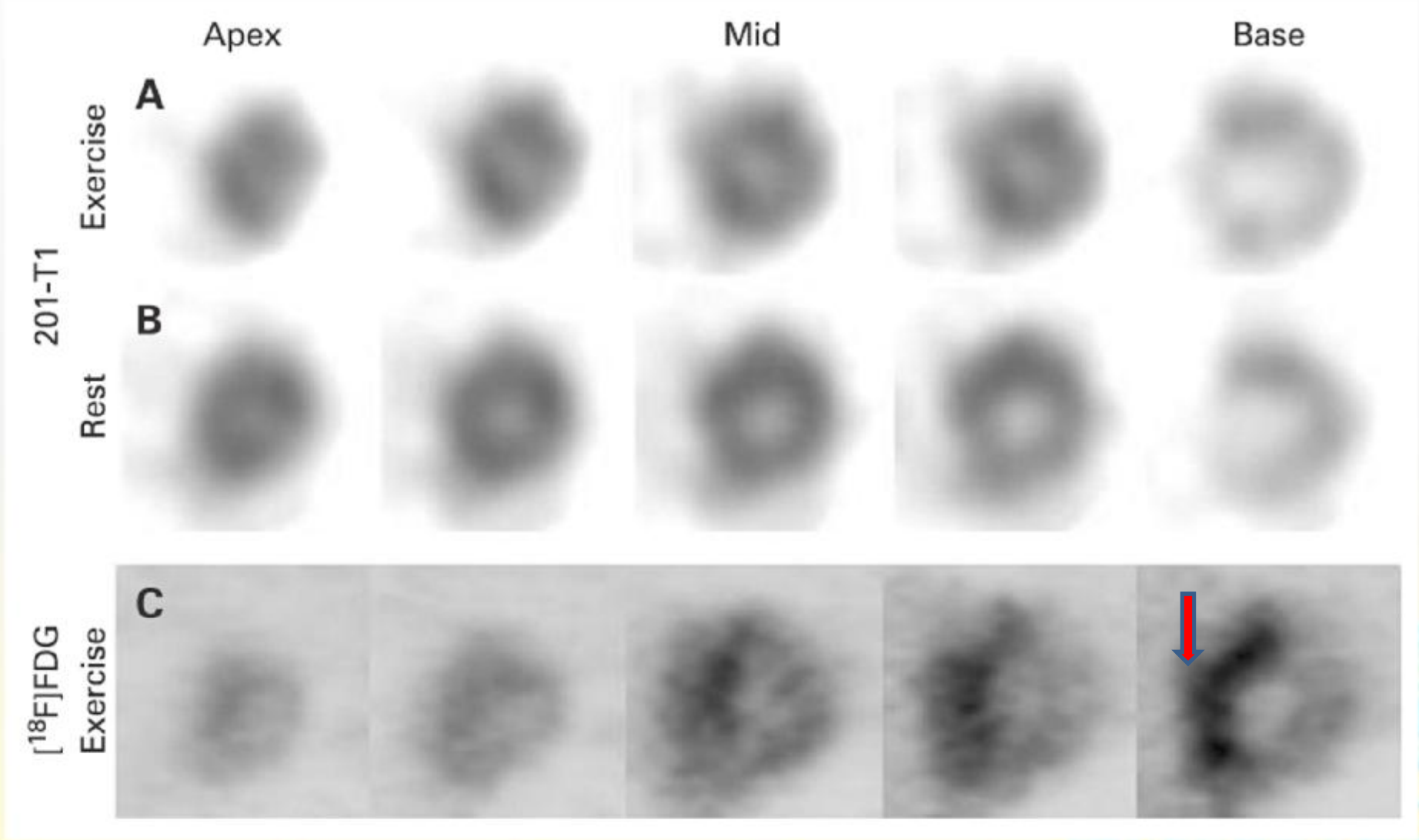

Yamano M, Heart 2009;95:1051

57-year-old man with a history of HCM

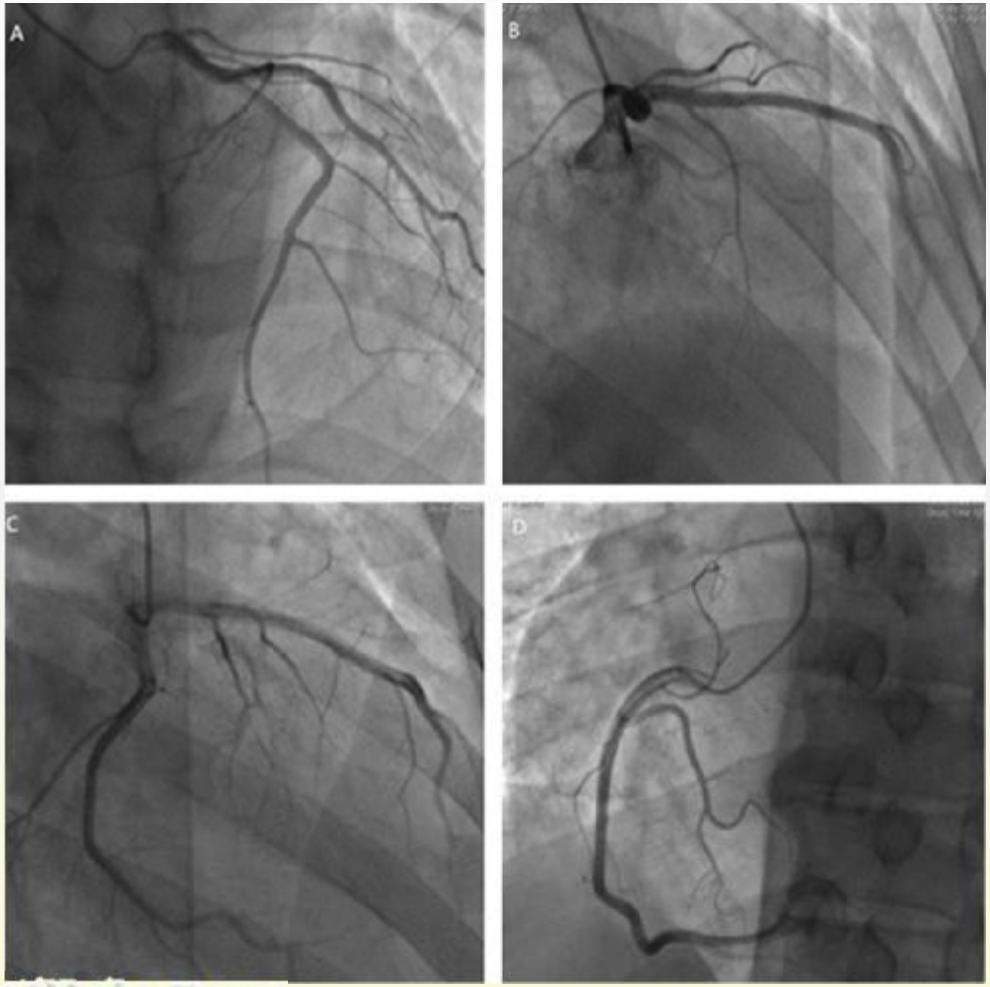

- **Atypical chest pain and dyspnoea in the past 6 months**
- **Family history of HCM**

Li S, et al. Clin Nucl Med 2017

Perfusion and Metabolism Imaging in HCM with MI but Normal Coronary Arteries

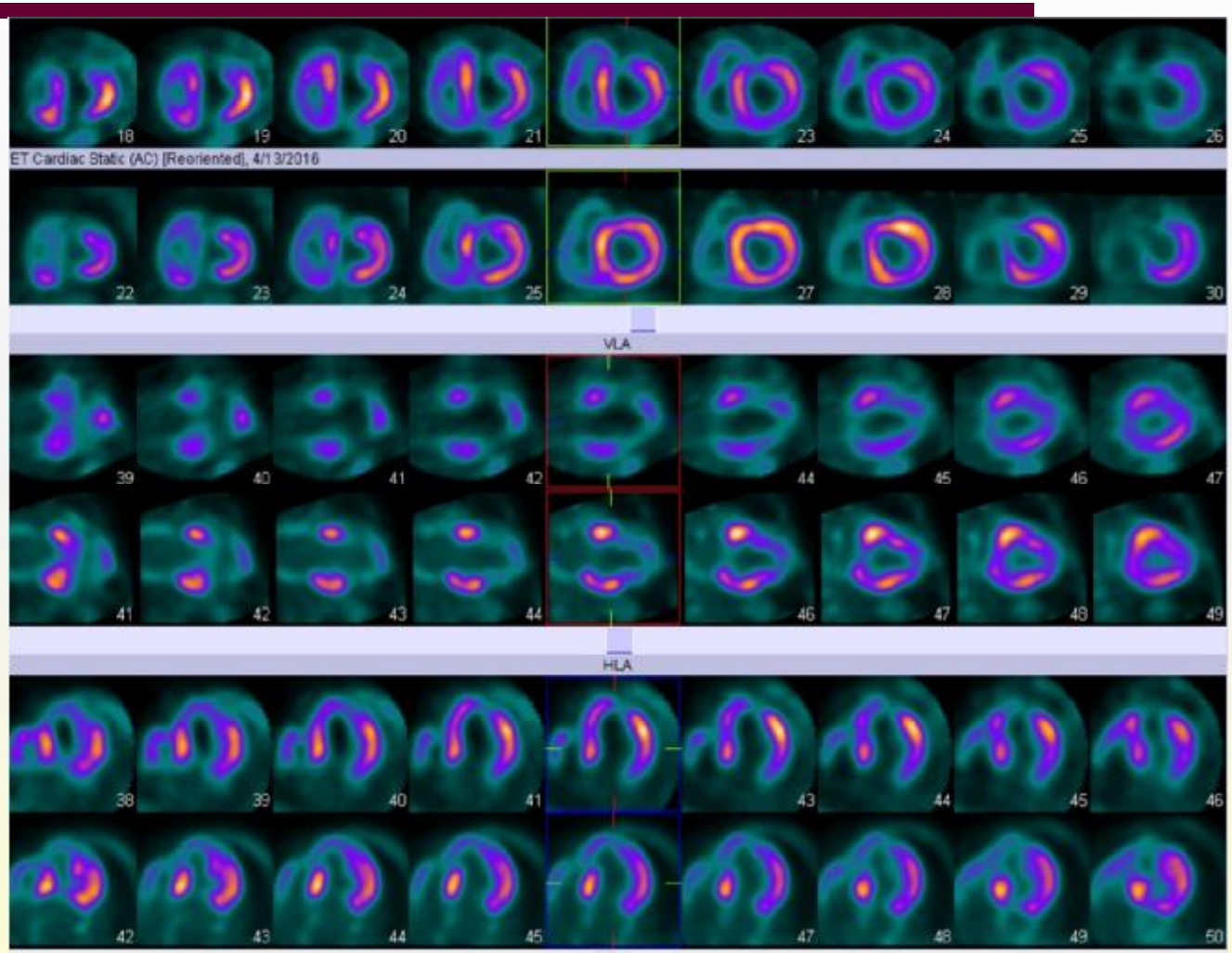

LVEF: 45%
EDV:173ml
ESV:95ml

Li SH, et al. Clin Nucl Med 2017

Isolated LV non-compaction
Female, 27-yrs-old, LVEF, 36%

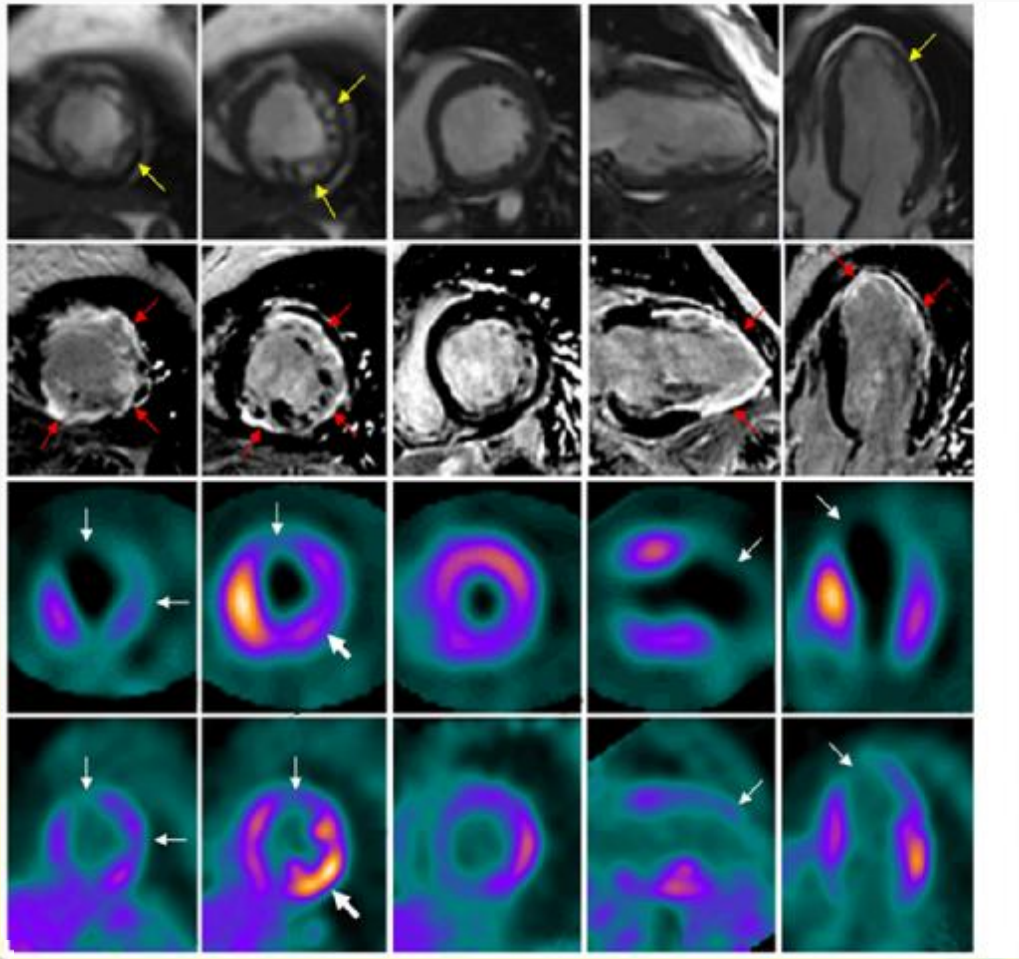

Gao XJ, et al. J Nucl Cardiol. 2014 Jun;21(3):633-42

Staging of cardiac sarcoidosis using resting myocardial perfusion scintigraphy (MPS), FDG-PET and LGE-CMR

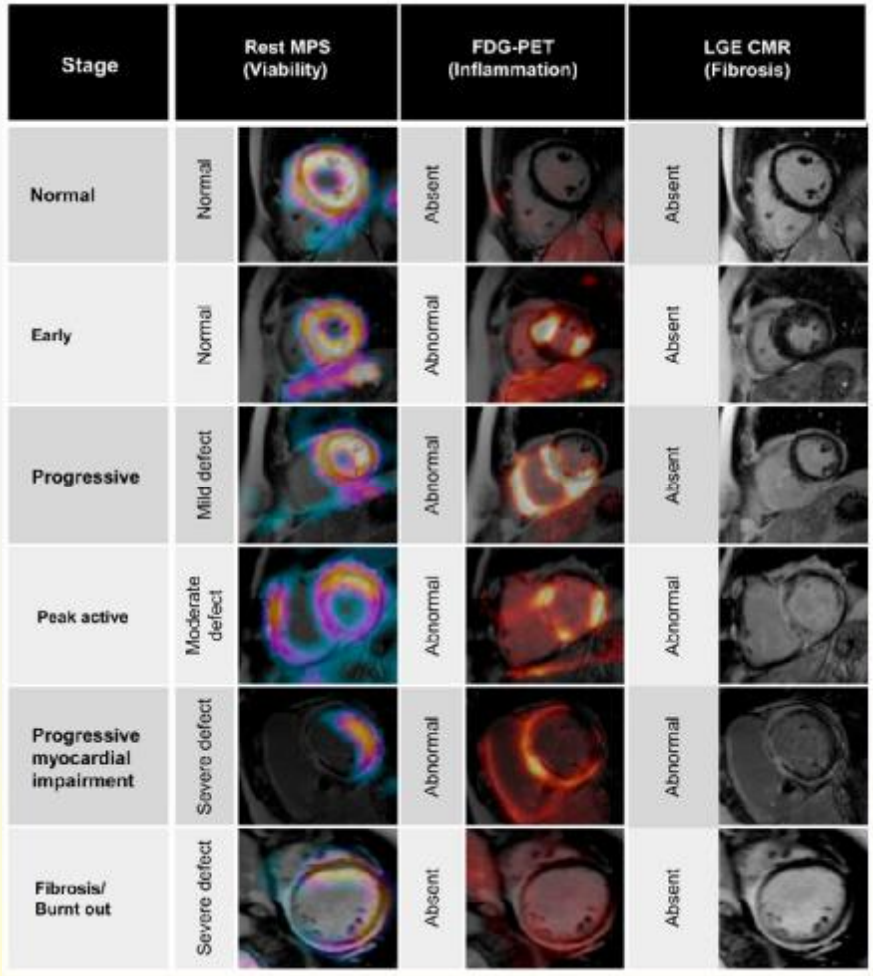

Okumura W., et al. J. Nucl. Med. 2004;45:1989–1998.

Increased F-18 FDG uptake in myocardial infarction

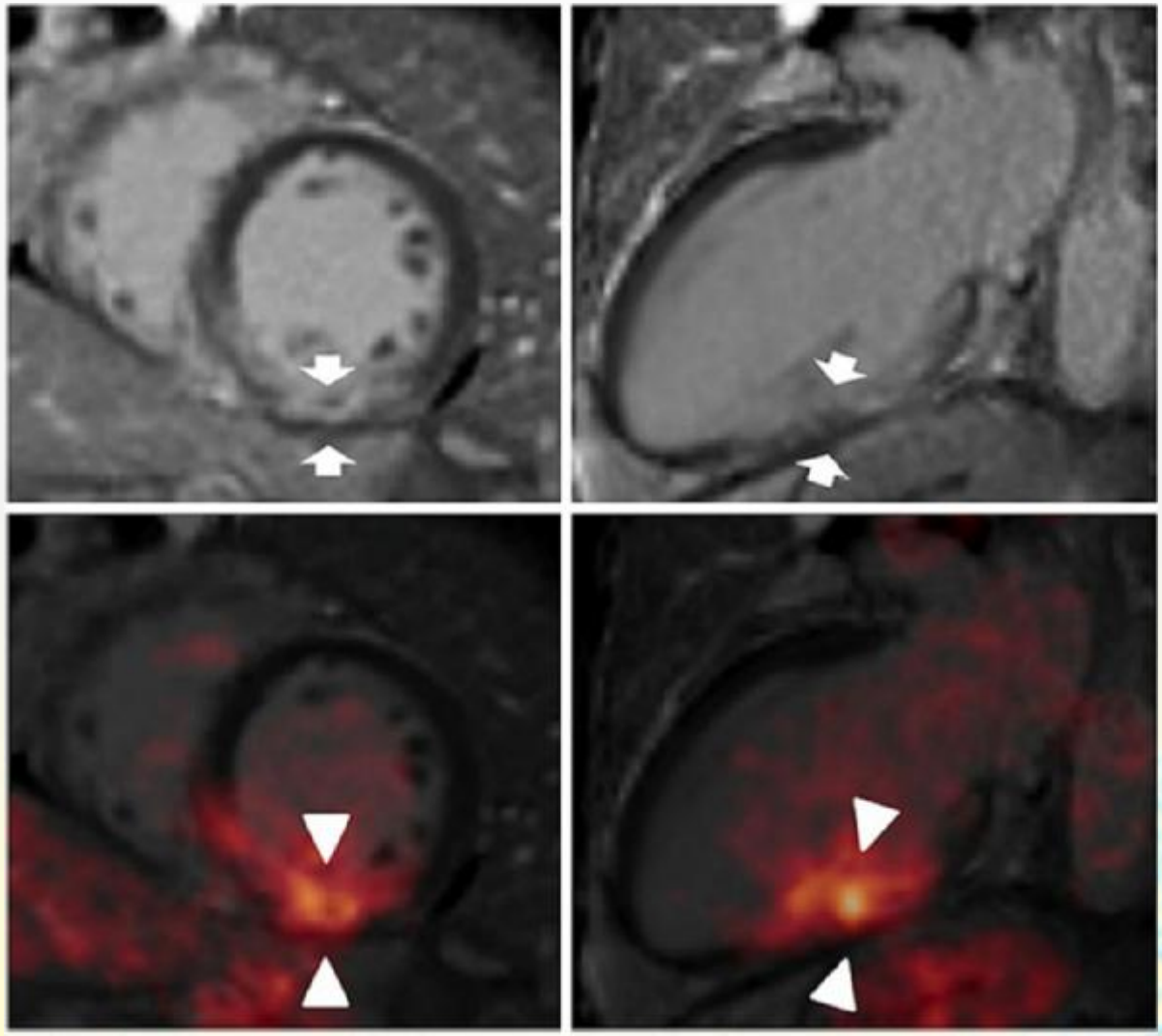

Rischpler C, et al. J Nucl Med. 2013;54:402–15

^{18}F-FDG PET/MRI of patient shortly after acute MI

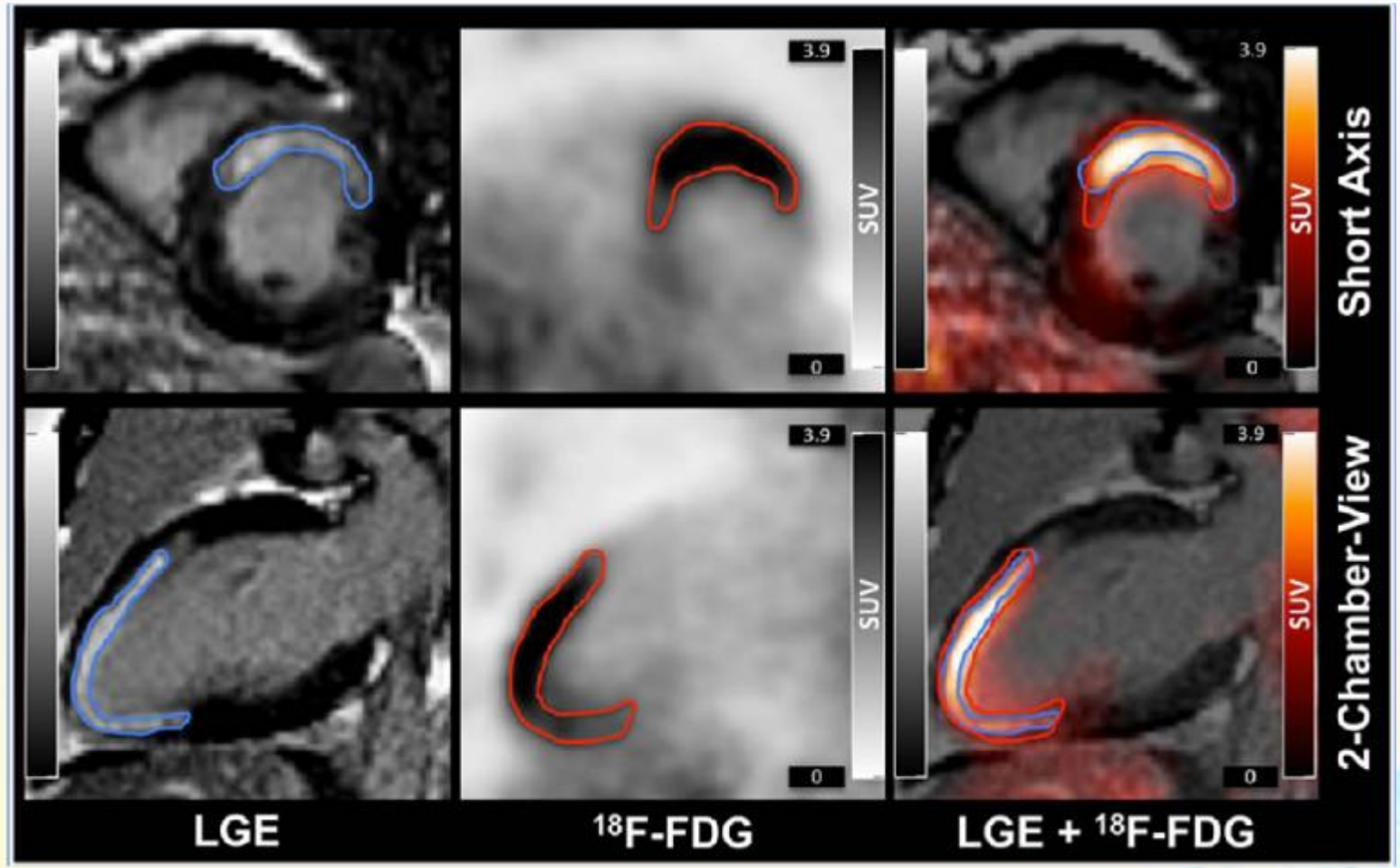

Rischpler et al. ***Circ Cardiovasc Imaging. 2016;9:e004316.***

Correlation between quantitative F-18-FDG extent and area at risk

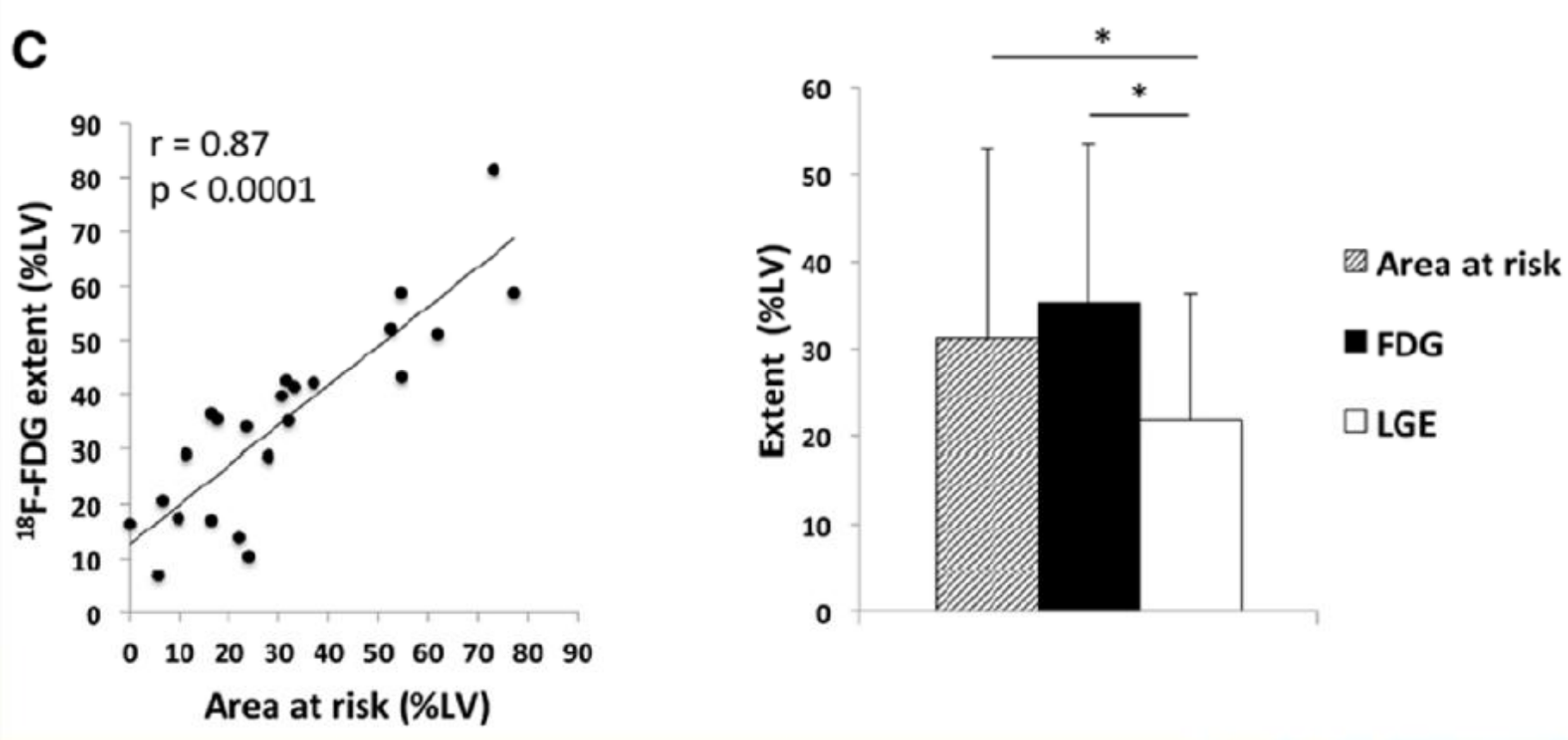

Rischpler et al. *Circ Cardiovasc Imaging. 2016;9:e004316.*

Atrial Uptake of FDG

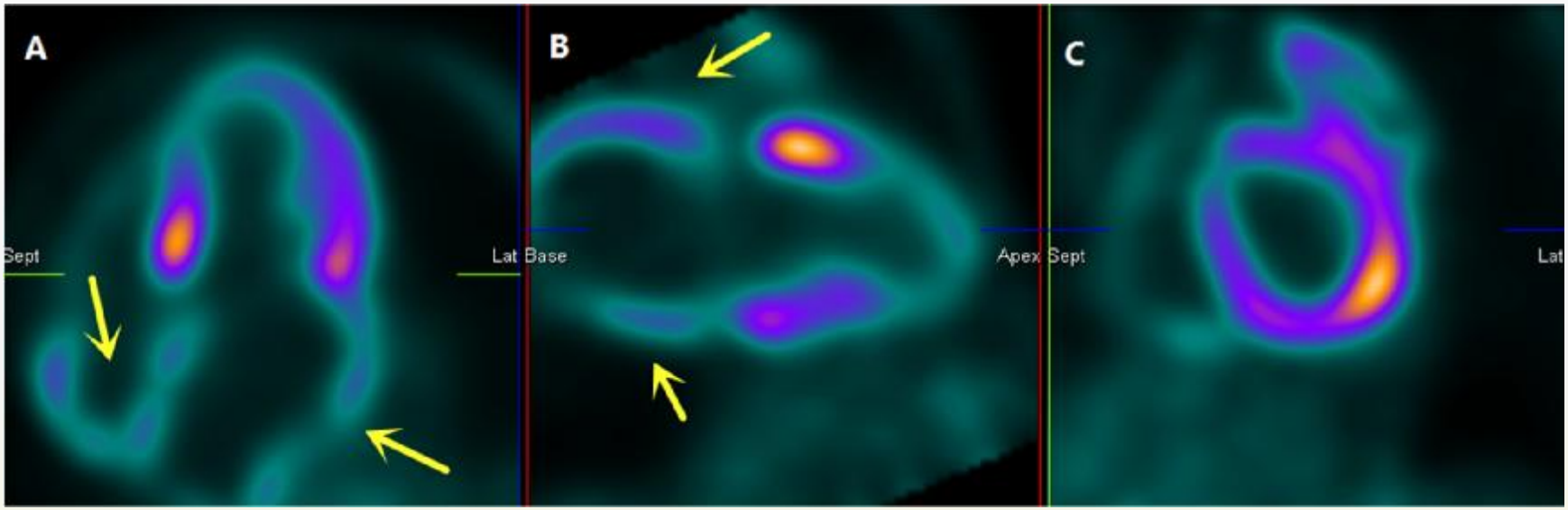

A 63-year-old man, who had chest congestion for 6 months and a 10-year history of rheumatic valvular heart disease

Unpublished data

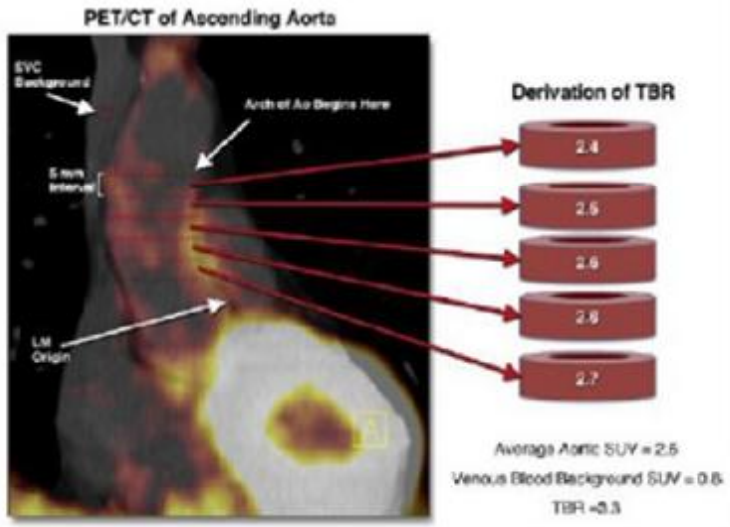

Measuring methods

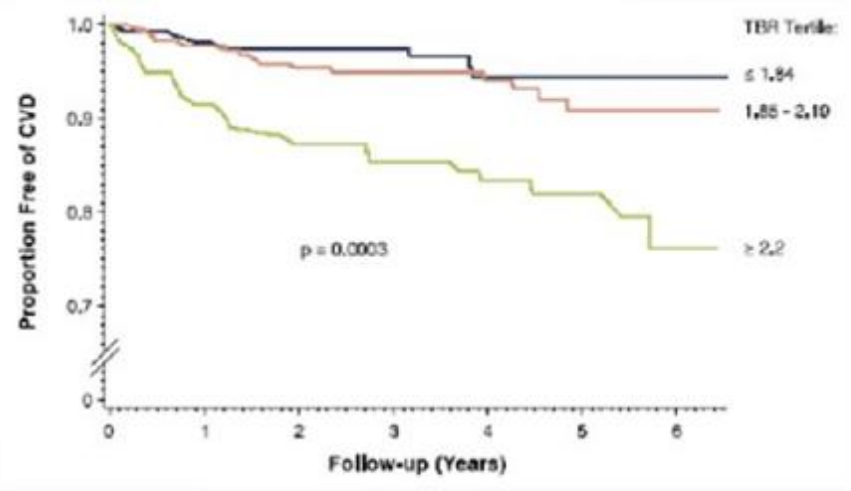

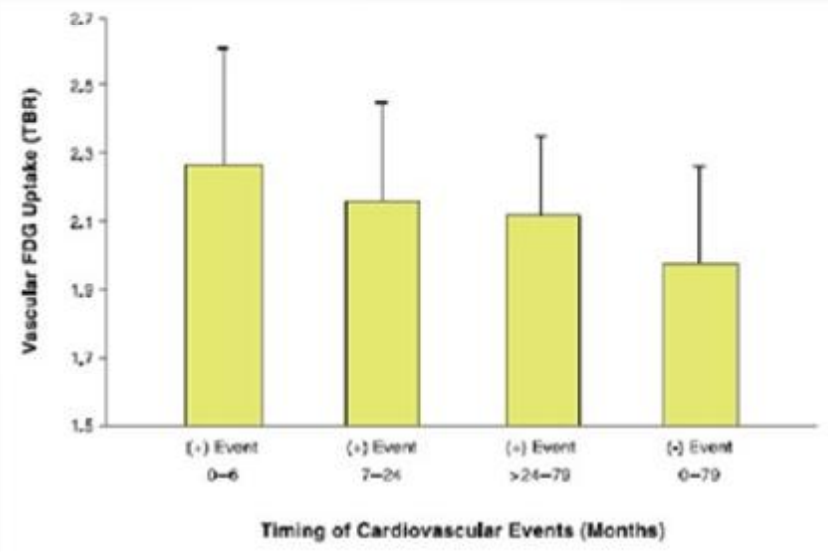

Figueroa AL et al. *JACC Cardiovasc Imaging* 2013;6:1250

^{18}F-fluoride PET for identification of ruptured and high-risk coronary atherosclerotic plaques

Study design:

- patients with MI (n=40) and stable angina (n=40) underwent ^{18}F-NaF and ^{18}F-FDG PET-CT, and invasive coronary angiography.
- ^{18}F-NaF uptake was compared with histology in carotid endarterectomy specimens from patients with symptomatic carotid disease, and with intravascular ultrasound in patients with stable angina.
- The primary endpoint was the comparison of ^{18}F-fluoride tissue-to-background ratios of culprit and non-culprit coronary plaques of patients with acute MI.

Joshi NV, et al. Lancet. 2014 Feb 22;383(9918):705-13.

PET/CT imaging of ^{18}F-fluoride and ^{18}F-FDG uptake in a patient with acute MI

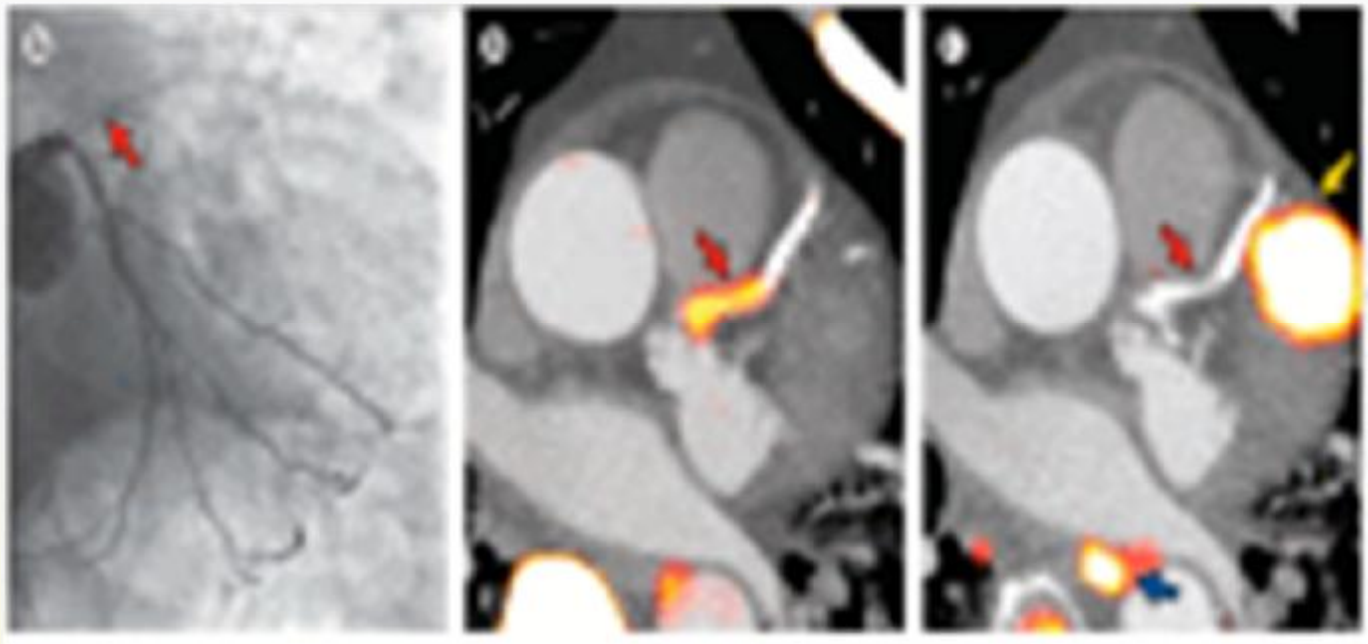

Oshi N.V., et al. Lancet. 2014;383:705–713.

^{18}F-Fluoride PET in Human

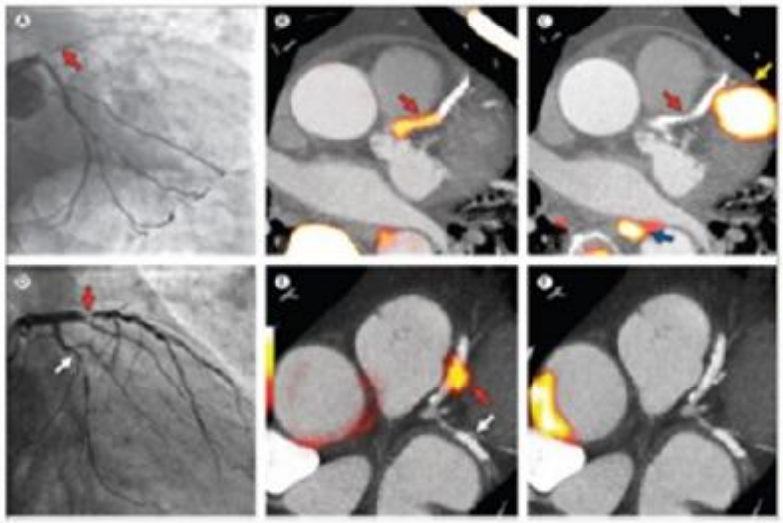

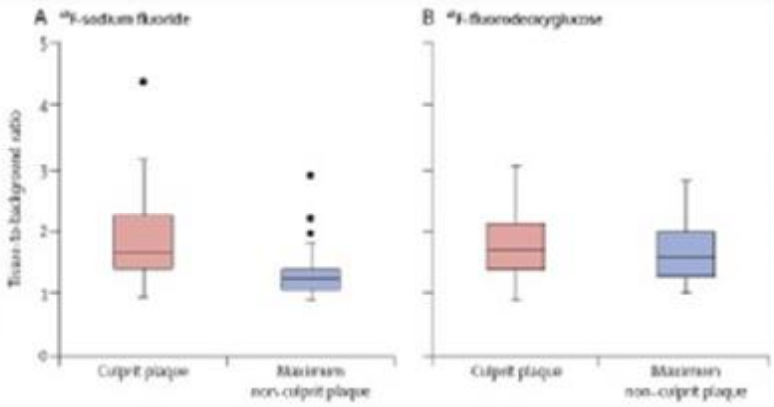

	^{18}F-fluoride positive plaques (n=15)	^{18}F-fluoride negative plaques (n=24)	p
Lumen			
Area (mm^2)	9·0 (5·7–13·5)	6·7 (4·7–9·7)	0·078
Minimal diameter (mm)	2·6 (1·7–3·1)	1·9 (1·7–2·6)	0·165
Maximum diameter (mm)	4·9 (4·1–5·3)	3·6 (3·1–4·6)	0·006
Vessel			
Area (mm^2)	24·1 (17·2–27·1)	14·5 (11·9–18·1)	0·002
Minimal diameter (mm)	4·4 (3·4–5·2)	3·6 (3·0–4·1)	0·057
Maximum diameter (mm)	6·5 (6·0–7·1)	5·2 (4·7–5·9)	0·0001
Plaque			
Length (mm)	14·2 (6·2–23·5)	15·2 (6·7–25·0)	0·941
Volume (mm^3)	152·9 (99·6–289·7)	91·0 (45·8–158·2)	0·032
Burden (%)*	55·6 (48·6–64·4)	54·2 (46·3–57·3)	0·174
Remodelling index	1·12 (1·09–1·19)	1·01 (0·94–1·06)	0·0004
Plaque composition			
Fibrous tissue (%)	51·0 (46·3–56·6)	58·1 (51·6–65·5)	0·015
Fibro-fatty (%)	10·9 (6·0–13·8)	12·6 (9·3–17·8)	0·092
Necrotic core (%)	24·6 (20·5–28·8)	18·0 (14·0–22·4)	0·001
Maximum frame necrotic core (%)†	35·5 (34·2–40·5)	29·2 (23·9–42·1)	0·009
Dense calcium (%)	12·6 (9·1–18·1)	10·2 (4·0–14·9)	0·092
Microcalcification, n (%)	11 (73%)	5 (21%)	0·002
Plaque classification, n (%)			
Thin-cap fibroatheroma	7 (47%)	4 (16%)	0·068
Thick-cap fibroatheroma	5 (33%)	9 (38%)	1·0
Pathological intimal thickening	0	7 (29%)	0·003
Fibrocalcific plaque	3 (20%)	4 (16%)	1·0

Joshi et al. *Lancet* 2014;383:705

^{18}F-fluoride PET for identification of ruptured and high-risk coronary atherosclerotic plaques

Interpretations:

- ^{18}F-NaF PET-CT is the first non-invasive imaging method to identify and localise ruptured and high-risk coronary plaque.

Joshi NV, et al. Lancet. 2014 Feb 22;383(9918):705-13.

CENTRAL ILLUSTRATION: Comparison Between ^{68}Ga-DOTATATE and [^{18}F] FDG Coronary PET Inflammation Imaging

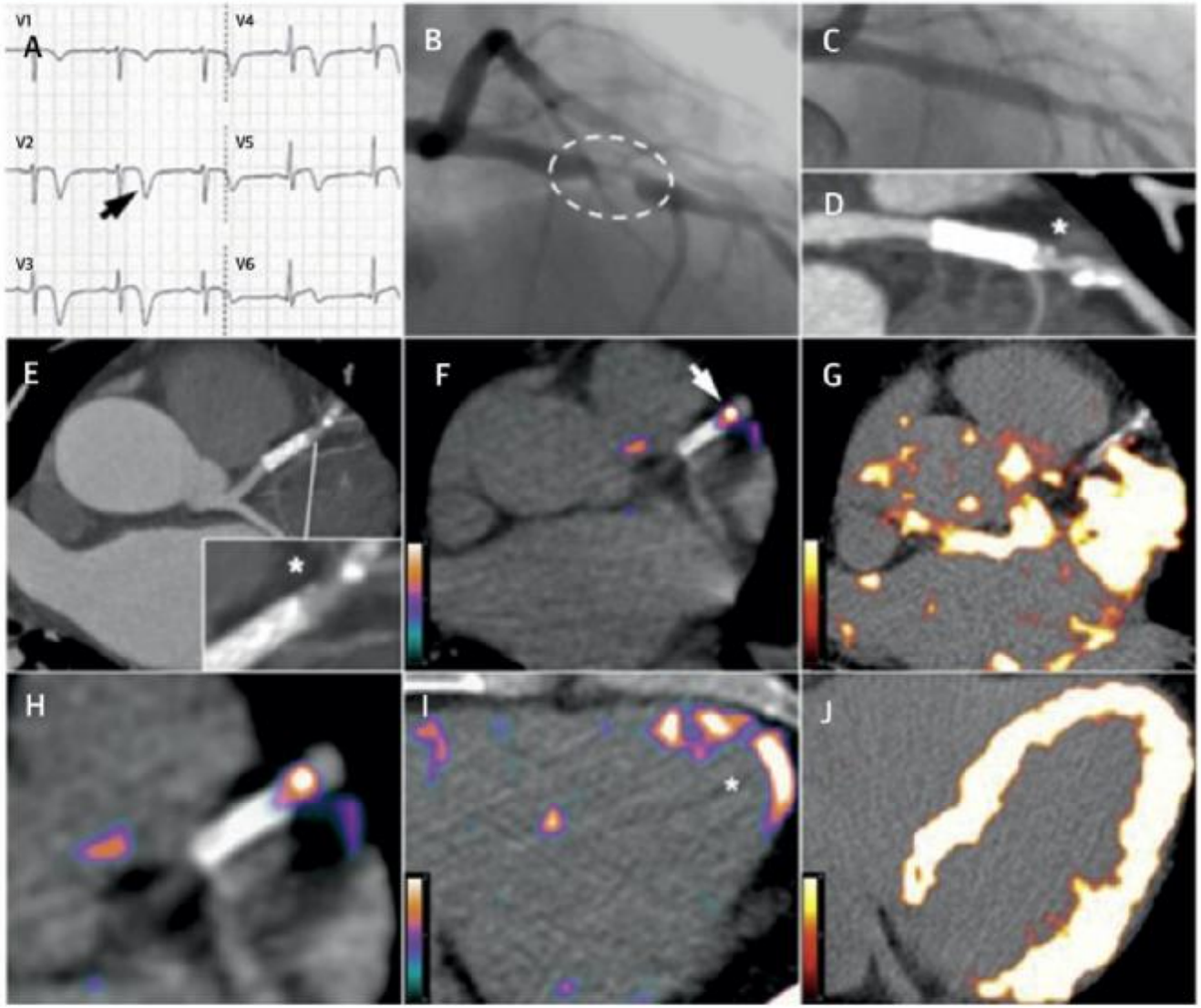

Tarkin, J.M. et al. J Am Coll Cardiol. 2017;69(14):1774-91.

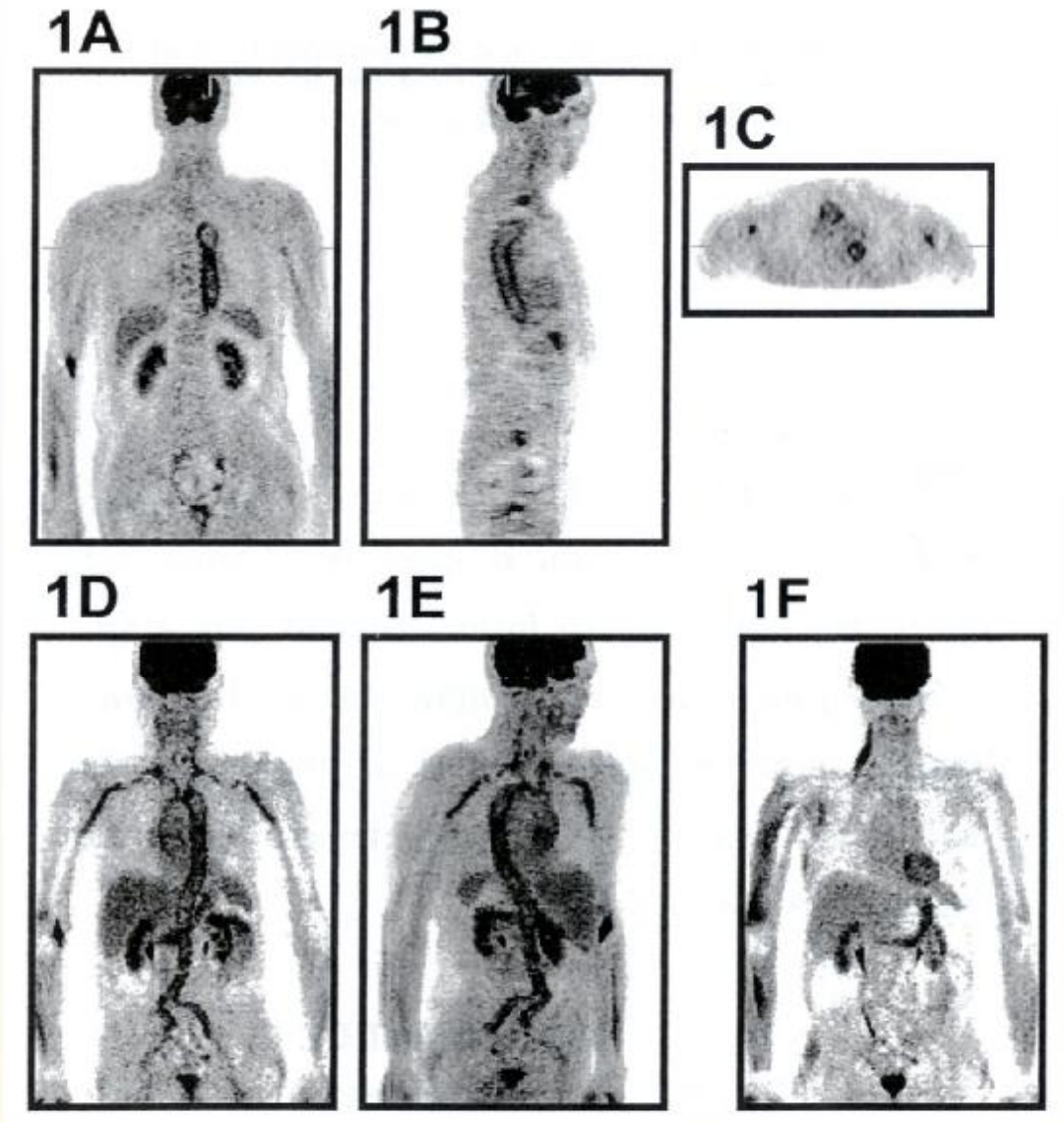

^{18}F-FDG-PET studies show increased ^{18}F-FDG uptake along the large vessel walls before, but not after, corticosteroid treatment. Pretreatment images with coronal, sagittal, and transaxial slices are shown in A, B, and C, respectively, and anterior view and right posterior oblique position are shown in D and E. F, Posttreatment control with anterior view.

Wenger, Circulation 2003,107:923

CENTRAL ILLUSTRATION Overview of Strategies to Overcome the Roadblocks in Cardiac Cell Therapy

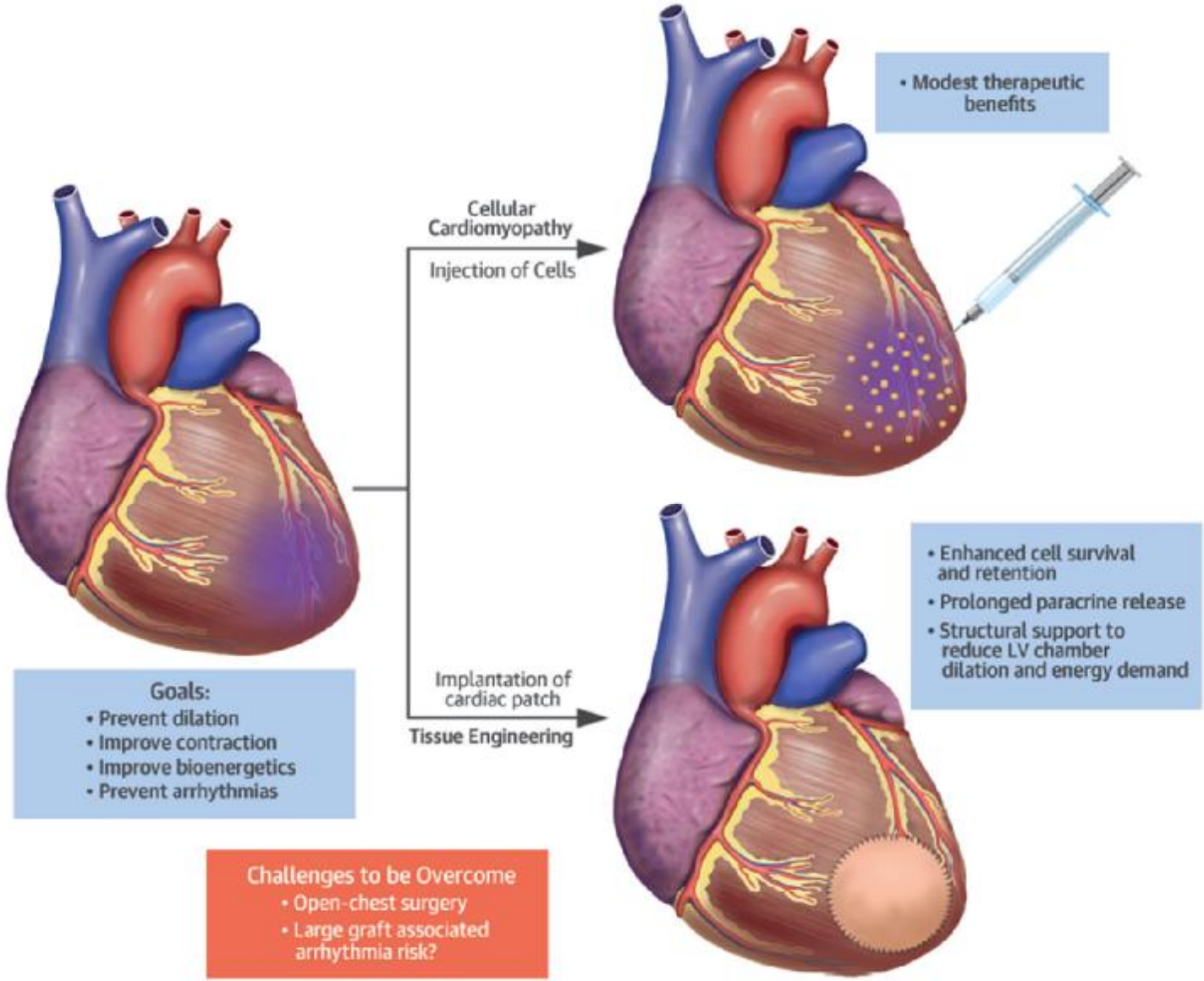

Yanamandala, M. et al. J Am Coll Cardiol. 2017;70(6):766–75.

Multimodality imaging in stem cell clinical trials

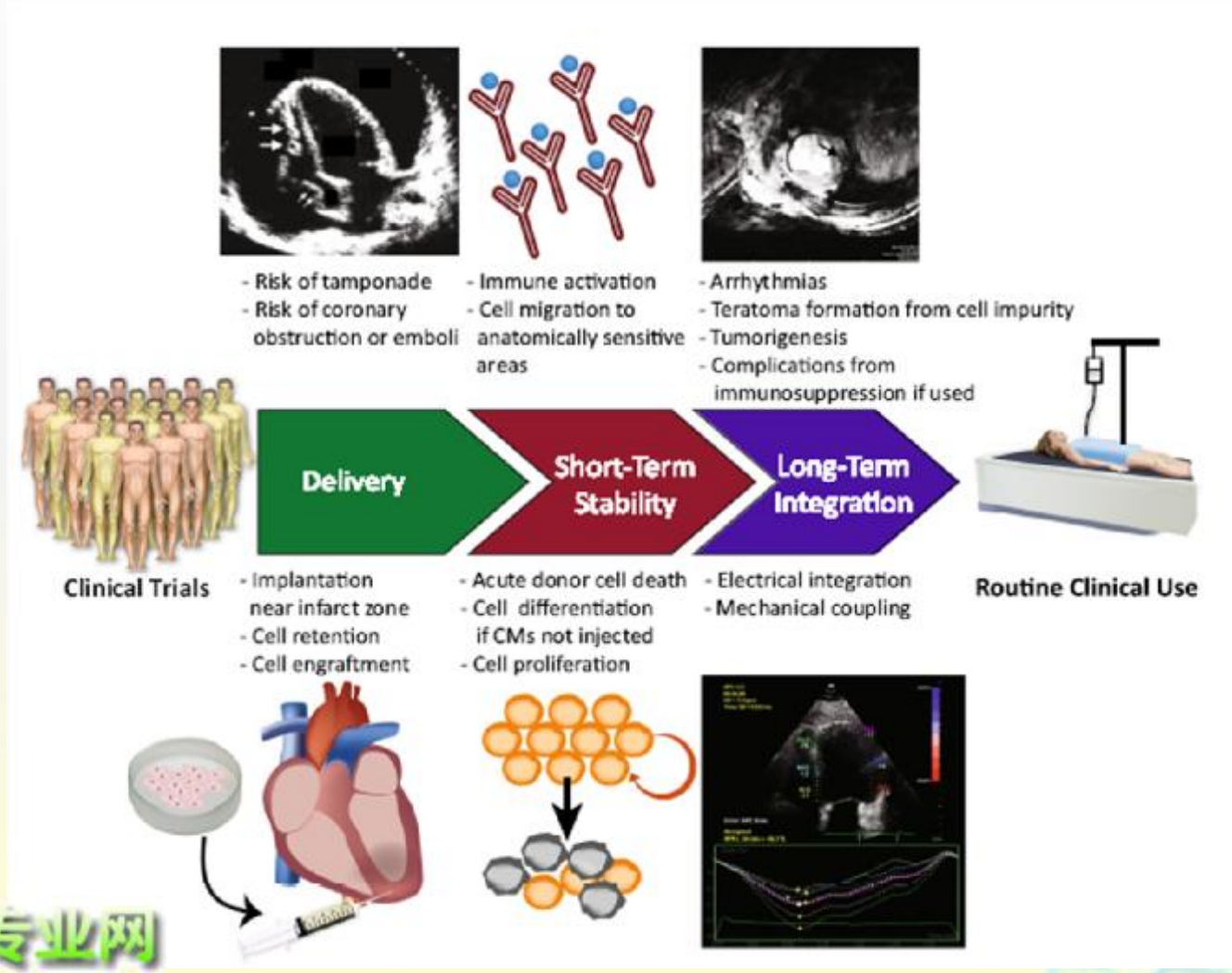

Vo and Nguyen Journal of Nuclear Cardiology 2017

Intramyocardial localization of F-18-FDG-labeled MNCs

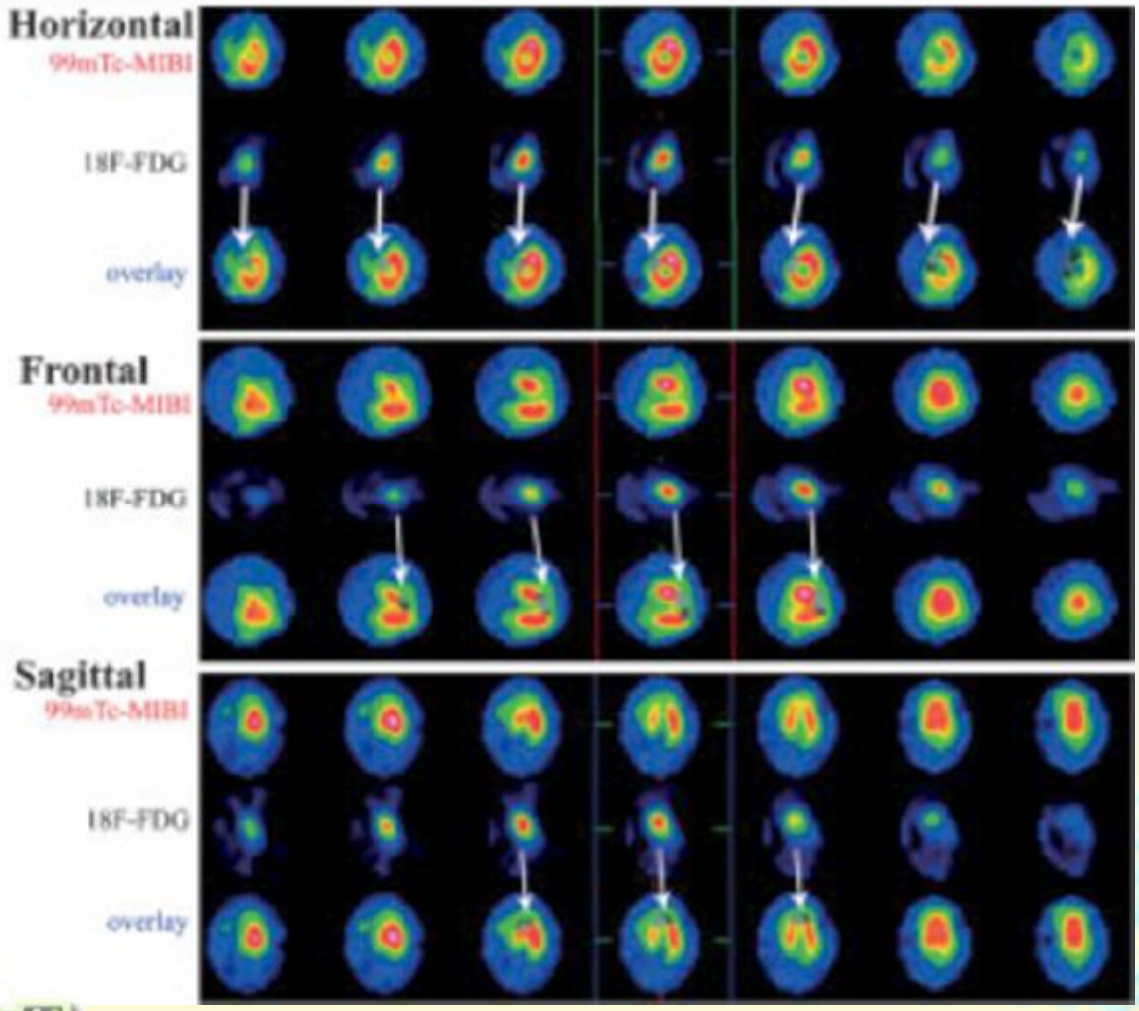

Qian HY, et al. Journal of Cellular Biochemistry 102:64–74 (2007)

FDG PET-CT images at week 1 and 4 in infarcted hearts receiving PBS versus MSCs

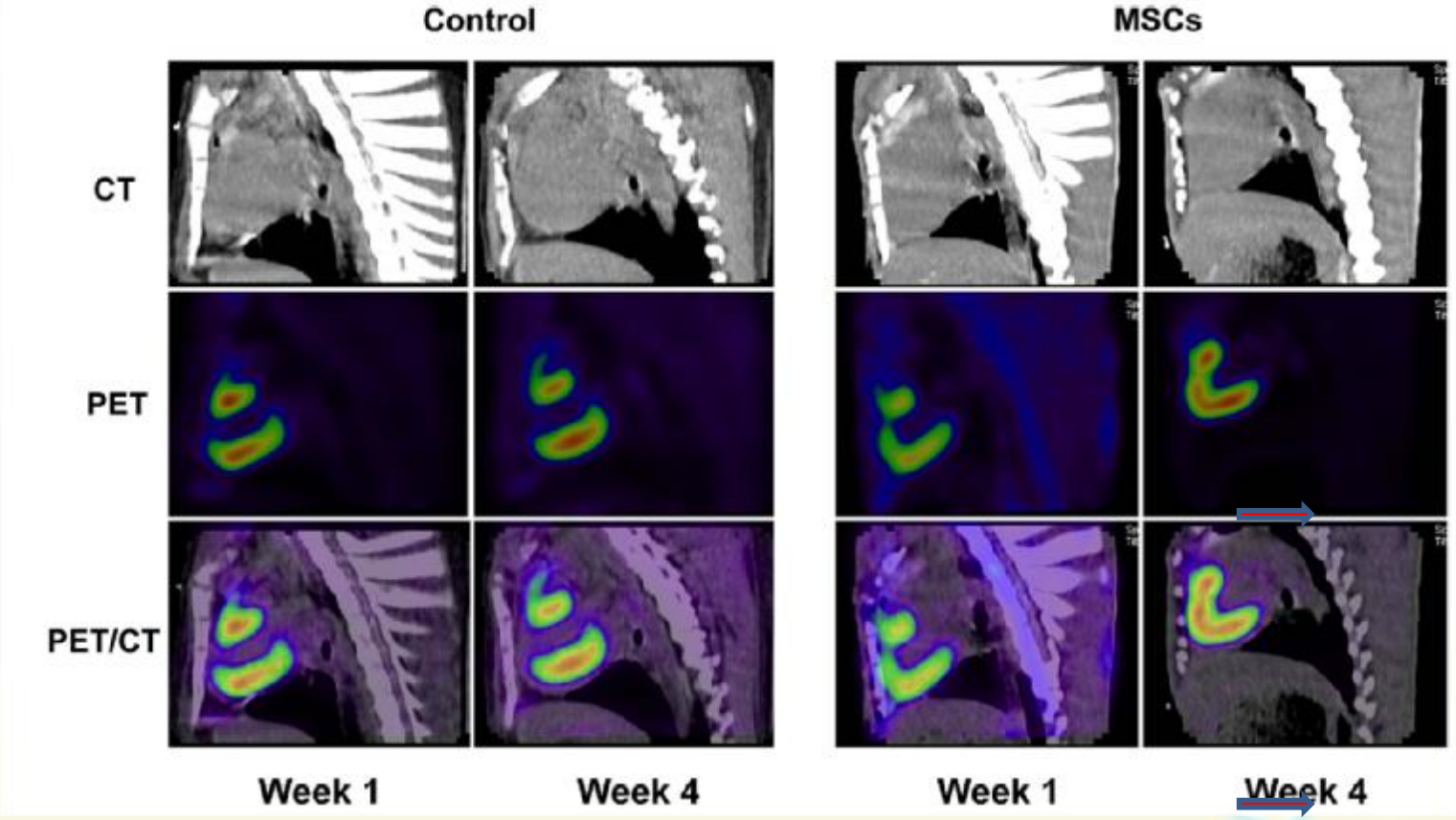

第三方评价：**Treatment with autologous bone marrow-derived MSCs can also promote cardiomyocyte survival by regulating glucose metabolism via the mechanistic target of Rapamycin pathway following MI (Bartczak et al. Curr Opin Organ Transplant 2017, 22:86–96)**

***Cai M, et al. Sci. Rep. 6, 28250; doi: 10.1038/*srep28250 (2016)**

心血管影像与心血管病学的协作

- 为临床诊断提供支持
  - 直接回答临床医师的问题
- 为疗效评价提供客观证据
- 与临床科室分享利益
  - 创造利润
  - 分享利润

拓展临床应用

- 针对临床病例，与临床科室沟通
- 针对临床问题，提供核医学解决方案
  - 优势
  - 不足
- 针对临床科研课题，应用核医学技术
  - 从临床科研到临床应用